



**UNIVERSIDAD DE INVESTIGACIÓN DE TECNOLOGÍA
EXPERIMENTAL YACHAY**

Escuela de Ciencias Químicas e Ingeniería

**TITULO: Inorganic Anticancer drugs based in iron and cobalt
complexes.**

Trabajo de integración curricular presentado como requisito para
la obtención de título como Químico

Autor:

Franco Jeanpierre Román Barragán

Tutor:

PhD. Juan Pablo Saucedo

Urcuquí, Mayo 2021

SECRETARÍA GENERAL
(Vicerrectorado Académico/Cancillería)
ESCUELA DE CIENCIAS QUÍMICAS E INGENIERÍA
CARRERA DE QUÍMICA
ACTA DE DEFENSA No. UITEY-CHE-2021-00019-AD

A los 29 días del mes de junio de 2021, a las 16:00 horas, de manera virtual mediante videoconferencia, y ante el Tribunal Calificador, integrado por los docentes:

Presidente Tribunal de Defensa	Dr. FERREIRA DE MENEZES AREIAS , FILIPE MIGUEL , Ph.D.
Miembro No Tutor	Dra. HIDALGO BONILLA, SANDRA PATRICIA , Ph.D.
Tutor	Dr. SAUCEDO VAZQUEZ, JUAN PABLO , Ph.D.

El(la) señor(ita) estudiante **ROMAN BARRAGAN, FRANCO JEANPIERRE**, con cédula de identidad No. **2350283723**, de la **ESCUELA DE CIENCIAS QUÍMICAS E INGENIERÍA**, de la Carrera de **QUÍMICA**, aprobada por el Consejo de Educación Superior (CES), mediante Resolución **RPC-SO-39-No.456-2014**, realiza a través de videoconferencia, la sustentación de su trabajo de titulación denominado: **INORGANIC ANTICANCER DRUGS BASED IN IRON AND COBALT COMPLEXES**, previa a la obtención del título de **QUÍMICO/A**.

El citado trabajo de titulación, fue debidamente aprobado por el(los) docente(s):

Tutor	Dr. SAUCEDO VAZQUEZ, JUAN PABLO , Ph.D.
--------------	---

Y recibió las observaciones de los otros miembros del Tribunal Calificador, las mismas que han sido incorporadas por el(la) estudiante.

Previamente cumplidos los requisitos legales y reglamentarios, el trabajo de titulación fue sustentado por el(la) estudiante y examinado por los miembros del Tribunal Calificador. Escuchada la sustentación del trabajo de titulación a través de videoconferencia, que integró la exposición de el(la) estudiante sobre el contenido de la misma y las preguntas formuladas por los miembros del Tribunal, se califica la sustentación del trabajo de titulación con las siguientes calificaciones:

Tipo	Docente	Calificación
Tutor	Dr. SAUCEDO VAZQUEZ, JUAN PABLO , Ph.D.	10,0
Miembro Tribunal De Defensa	Dra. HIDALGO BONILLA, SANDRA PATRICIA , Ph.D.	10,0
Presidente Tribunal De Defensa	Dr. FERREIRA DE MENEZES AREIAS , FILIPE MIGUEL , Ph.D.	10,0

Lo que da un promedio de: **10 (Diez punto Cero)**, sobre 10 (diez), equivalente a: **APROBADO**

Para constancia de lo actuado, firman los miembros del Tribunal Calificador, el/la estudiante y el/la secretario ad-hoc.

Certifico que en cumplimiento del Decreto Ejecutivo 1017 de 16 de marzo de 2020, la defensa de trabajo de titulación (o examen de grado modalidad teórico práctica) se realizó vía virtual, por lo que las firmas de los miembros del Tribunal de Defensa de Grado, constan en forma digital.

ROMAN BARRAGAN, FRANCO JEANPIERRE
Estudiante

FILIPE MIGUEL
 FERREIRA DE
 MENEZES AREIAS

Firmado digitalmente por FILIPE
 MIGUEL FERREIRA DE MENEZES
 AREIAS
 Fecha: 2021.07.08 22:16:25 -05'00'

Dr. FERREIRA DE MENEZES AREIAS , FILIPE MIGUEL , Ph.D.
Presidente Tribunal de Defensa

JUAN
PABLO
SAUCEDO
VAZQUEZ

Firmado digitalmente por
JUAN PABLO
SAUCEDO
VAZQUEZ
Fecha: 2021.07.08
08:00:15 -05'00'

Dr. SAUCEDO VAZQUEZ, JUAN PABLO , Ph.D.
Tutor

SANDRA PATRICIA
HIDALGO BONILLA

Firmado digitalmente por SANDRA
PATRICIA HIDALGO BONILLA
Fecha: 2021.07.07 17:38:26 -05'00'

Dra. HIDALGO BONILLA, SANDRA PATRICIA , Ph.D.
Miembro No Tutor

CARLA SOFIA
YASELGA NARANJO

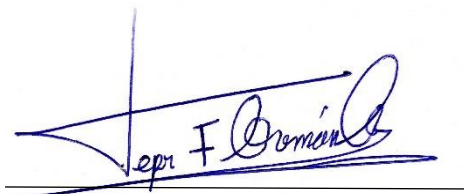
Digitally signed by CARLA SOFIA
YASELGA NARANJO
Date: 2021.07.07 17:30:35 -05'00'

YASELGA NARANJO, CARLA
Secretario Ad-hoc

AUTORÍA

Yo, **FRANCO JEANPIERRE ROMÁN BARRAGÁN**, con cédula de identidad 2350283723, declaro que las ideas, juicios, valoraciones, interpretaciones, consultas bibliográficas, definiciones y conceptualizaciones expuestas en el presente trabajo; así como, los procedimientos y herramientas utilizadas en la investigación, son de absoluta responsabilidad del autor del trabajo de integración curricular. Así mismo, me acojo a los reglamentos internos de la Universidad de Investigación de Tecnología Experimental Yachay.

Urcuquí, Mayo 2021.



Franco Jeanpierre Román Barragán

C.I.: 2350283723

AUTORIZACIÓN DE PUBLICACIÓN

Yo, **FRANCO JEANPIERRE ROMÁN BARRAGÁN**, con cédula de identidad 2350283723, cedo a la Universidad de Tecnología Experimental Yachay, los derechos de publicación de la presente obra, sin que deba haber un reconocimiento económico por este concepto. Declaro además que el texto del presente trabajo de titulación no podrá ser cedido a ninguna empresa editorial para su publicación u otros fines, sin contar previamente con la autorización escrita de la Universidad.

Asimismo, autorizo a la Universidad que realice la digitalización y publicación de este trabajo de integración curricular en el repositorio virtual, de conformidad a lo dispuesto en el Art. 144 de la Ley Orgánica de Educación Superior.

Urcuquí, Mayo 2021.



Franco Jeanpierre Román Barragán

C.I.: 2350283723

DEDICATORIA

Dedicado para toda mi familia que confió en mí al partir a este gran reto. A mis padres y hermanas que aportaron mucho en este logro, y a mis sobrinos para que se motiven a conseguir grandes cosas.

AGRADECIMIENTO

Mis más sinceros agradecimientos a mi familia, en especial a mi madre que ha sido un pilar fundamental en la búsqueda de este y todos mis logros, a mi padre que estuvo pendiente en este camino, así también a mis hermanas que supieron apoyarme de una u otra forma para no rendirme en los retos que me he puesto. A todos los amigos y compañeros que hice en la Universidad y que fueron un gran apoyo desde el comienzo de la que fue una nueva etapa, agradeciendo también la posibilidad de poder encontrar tan buenas personas.

Finalmente, también quiero extender un gran agradecimiento a todos los profesores que tuve la oportunidad de conocer y me motivaron en este camino, en especial a mi tutor Juan Pablo que me supo guiar de gran manera en este trabajo y motivar en todas las materias que recibí.

Resumen

El estudio de compuestos de coordinación con fines terapéuticos ha ido en aumento debido a las grandes potencialidades que estos presentan por su capacidad de interacción con biomoléculas y debido a los interesantes mecanismos de reacción que llevan a cabo para sus funciones y que en muchos casos no se han aprovechado completamente. Por lo anterior, son necesarios más estudios en nuevos complejos metálicos en torno a mecanismos de acción que permitan el desarrollo de nuevos medicamentos hacia enfermedades celulares o teniendo como objetivo moléculas específicas de nuestro cuerpo para lograr atacar graves enfermedades como el cáncer, que afectan a la sociedad a nivel mundial. En este trabajo, se plantea el uso de complejos metálicos anticancerígenos con menor toxicidad para el organismo que la que presenta el ya conocido cisplatino. En este contexto, se propone sintetizar compuestos de coordinación con metales como el cobalto y el hierro, que buscan actuar con el ADN (ácido desoxirribonucleico) ya sea mediante un mecanismo similar al cisplatino (unión covalente a biomoléculas), o por interacciones de apilamiento π a través de anillos aromáticos presentes en los ligantes. Así, se obtuvieron dos complejos de cobalto(III), uno con geometría octaédrica y otro con geometría tetraédrica, y dos complejos de hierro(III) con geometría octaédrica, a estos se les coordinaron los ligantes tipo bases de Schiff con anillos aromáticos para aprovechar las interacciones de apilamiento π . Se obtuvieron resultados alentadores de la interacción de dos estos complejos con ADN de origen vegetal, esta interacción (intercalación) fue evaluada mediante espectroscopia UV-Vis (Ultravioleta-Visible) y simulada con software para docking como Autodock4 y Hex 8.0.0.

Palabras clave: bases de Schiff, compuestos de coordinación, cisplatino, interacciones de apilamiento π , docking.

Abstract

The study of coordination compounds with therapeutic purposes has been increasing due to the great potentialities that they have and by the capacity of interaction with biomolecules, and by the interesting mechanisms of reaction that carry out in their functions, which in many cases have not been fully exploited. For the last, more studies in new metal complexes are necessary around mechanisms of action that allow the development of new drugs against cellular diseases or targeting specific molecules of our body to attack serious diseases as cancer that affect society worldwide. In this work, the use of anticancer metal complexes with less toxicity to the body than so-called cisplatin is proposed. In this context, it is proposed to synthesize coordination compounds with metals such as cobalt and iron, which try to act with a DNA (deoxyribonucleic acid) either through a mechanism similar to cisplatin (covalent binding to biomolecules) or by π stacking interactions through aromatic rings present in the ligands. So, two cobalt (III) complexes were obtained, one with octahedral geometry and the other with tetrahedral geometry, and two of iron (III) complexes with octahedral geometry, in these were added Schiff base-type ligands with aromatic rings to take advantage of π stacking interactions. The obtained results were interesting to the interaction of two these complexes with vegetal-based DNA, this interaction (intercalation) was evaluated with UV-Vis (Ultraviolet-Visible) spectroscopy, and simulated with docking software as AutoDock4 and Hex 8.0.0.

Keywords: Schiff-bases, coordination compounds, cisplatin, π -stacking interaction, docking.

Contents

Introduction	1
CHAPTER 1: Theoretical Framework	8
1.1. Coordination compounds.....	8
1.2. Medicinal coordination compounds	8
1.3. Schiff bases ligands.....	9
1.4. Cobalt complexes	10
1.5. Iron complexes	10
1.6. Mechanism of action from metal-based drugs.....	11
1.6.1 Covalent binding of metal-based drugs to biomolecules.....	11
1.7. π - π stacking interactions.....	13
1.8. Electronic states in Metal Complexes	14
1.8.1. Metal Centred (MC) or d-d transitions.....	14
1.8.2. Charge transference (CT) or optical electron transfer transitions	14
1.8.3. Ligand centered (LC) or intra-ligand transitions.....	15
1.9. DNA concentration and purity	15
1.9.1. DNA-drug interactions measurements	15
1.10. Docking Simulations	16
1.10.1 Autodock software	17
1.10.2 Hex 8.0.0 software	17
CHAPTER 2: Methodology	18
2.1. Reagents.....	18
2.2. Laboratory Equipment	19
2.3. Cinnamaldehyde extraction	19
2.4. Synthesis of Ligands	19
2.5. Synthesis of $[\text{Fe}(\text{DMSO})_6](\text{NO}_3)_3$	20
2.6. Synthesis of Complexes.....	20
2.6.1. Synthesis of the Cobalt (III) complex with the ligand derivate from <i>p</i> -anisaldehyde.	20
2.6.2. Synthesis of the Cobalt (III) complex with the ligand derivate from cinnamaldehyde.....	20
2.6.3. Synthesis of the Iron (III) complex with the ligand derivate from <i>p</i> -anisaldehyde.	20

2.6.4.	Synthesis of the Iron (III) complex with the ligand derivate from cinnamaldehyde.	21
2.7.	Phosphate-buffered saline (PBS) preparation	21
2.8.	Vegetable DNA extraction	21
2.9.	DNA interaction with complexes	21
2.10.	Characterization techniques	22
2.10.1.	Infrared Spectroscopy (IR)	22
2.10.2.	UV-Vis Spectroscopy	22
2.10.3.	Magnetic Susceptibility	22
2.11.	Docking studies of ligands-DNA with Autodock4	22
2.12.	Docking studies of complexes-DNA interactions with Hex 8.0.0 software	23
CHAPTER 3: Results and discussion		24
3.1.	Cinnamaldehyde extraction	24
3.1.1.	Infrared spectroscopy of Cinnamaldehyde	25
3.2.	Synthesis of Ligands	25
3.3.	Cobalt complex with ligand based on <i>p</i> -anisaldehyde (complex 1).	29
3.3.1	Characterization of complex 1 by magnetic susceptibility	30
3.3.2.	Crystal Field Theory of complex 1.	31
3.3.3.	Infrared studies of complex 1	32
3.3.4.	UV-Vis Spectroscopy of complex 1	33
3.3.5.	Remarks of proposed structures	34
3.3.6	DNA extraction	34
3.3.7	DNA binding with the complex 1.	35
3.4.	Cobalt complex with ligand based on cinnamaldehyde (complex 2).	36
3.4.1.	Characterization of complex 2 by magnetic susceptibility	37
3.4.2.	Crystal Field Theory	38
3.4.3.	Infrared spectroscopy of complex 2	40
3.4.4.	UV-Vis Spectroscopy of complex 2	41
3.4.5.	Remarks of proposed structures	42
3.4.6.	DNA binding with the complex 2.	43
3.5.	Iron complex with ligand based on <i>p</i> -anisaldehyde (complex 3).	44
3.5.1.	Characterization of complex 3 by magnetic susceptibility	44
3.5.2.	Crystal Field Theory	45
3.5.3.	Infrared spectroscopy of complex 3	46
3.5.4.	UV-Vis Spectroscopy of complex 3	47
3.5.5.	Remarks of proposed structures	48

3.5.6.	DNA binding with the complex	48
3.6.	Iron complex with ligand based on cinnamaldehyde (complex 4).....	49
3.6.1.	Characterization of complex 4 by magnetic susceptibility.....	50
3.6.2.	Crystal Field Theory	51
3.6.3.	Infrared spectroscopy of complex 4.....	52
3.6.4.	UV-Vis Spectroscopy of complex 4.....	53
3.6.5.	Remarks of proposed structures.....	53
3.6.6.	DNA binding with the complex	54
3.7.	Docking studies of synthesized ligands using Autodock software	55
3.7.1.	Interaction with ligand based on <i>p</i> -anisaldehyde.....	55
3.7.2.	Interaction with ligand based on cinnamaldehyde.....	56
3.8.	Docking studies of synthesized complexes using Hex 8.0.0 software.	58
3.8.1.	Cobalt complex with ligand based on <i>p</i> -anisaldehyde (complex 1).....	58
3.8.2.	Cobalt complex with ligand based on cinnamaldehyde (complex 2).....	58
3.8.3.	Iron complex with ligand based on <i>p</i> -anisaldehyde (complex 3).....	59
3.8.4.	Iron complex with ligand based on cinnamaldehyde (complex 4).....	60
	Conclusions	61
	Recommendations	63
	Perspectives	63
	References.....	64
	ANNEXES	73

LIST OF FIGURES

Figure 1. Molecular docked structure of ligand-L complexed with B-DNA. A) Molecular surface view interaction of ligand with DNA. B) Hydrogen bonding interaction of ligand with DNA (PDB ID:1BNA). Taken from Khan. ²⁹	5
Figure 2. Scheme of Schiff base condensation mechanism from amines.	10
Figure 3. Scheme of mechanism of binding between DNA and cisplatin, taken from Alderden. ¹⁶	12
Figure 4. Major types of cisplatin adducts produced by binding of cisplatin with DNA taken from Kelland. ²⁰	13
Figure 5. Main orientations of aromatic-aromatic interactions taken from Janiak. ³⁸	14
Figure 6. Simple distillation system used in the extraction of cinnamaldehyde.	24
Figure 7. Cinnamaldehyde obtained.	24
Figure 8. IR spectrum of the extracted cinnamaldehyde.	25
Figure 9. Mechanism of formation of proposed ligands.	26
Figure 10. Change of color after addition of acid.	27
Figure 11. Scheme of reaction between p-anisaldehyde with ethylenediamine.	27
Figure 12. TLC plate of only p-anisaldehyde (C), and the ligand based on p-anisaldehyde (L1).	28
Figure 13. Scheme of reaction between cinnamaldehyde with ethylenediamine.	28
Figure 14. TLC plate of only cinnamaldehyde (C), and the ligand based on cinnamaldehyde (L1).	29
Figure 15. Synthesized complex of cobalt(III) with p-anisaldehyde.	29
Figure 16. a) and b) are proposed structures of Complex 1.	30
Figure 17. Octahedral Crystal Field of complex 1.	31
Figure 18. Tuning of cobalt redox potential by substitution of water for amine (L) ligands.	32
Figure 19. IR spectrum of complex 1.	33
Figure 20. UV-Vis spectrum of complex 1. Insert: Spectrum of complex 1 in range 350-700nm.	33
Figure 21. Vegetable DNA extracted.	35
Figure 22. UV-Vis Spectrum of vegetable DNA	35
Figure 23. UV-Vis spectrum of cobalt(III) complex 1, blue line represents the only metal complex signal and red line shows the increases in amount of DNA.	36
Figure 24. Synthesized complex of cobalt(III) with cinnamaldehyde.	36
Figure 25. a) and b) are proposed structures of complex 2.	37
Figure 26. Tetrahedral Crystal Field of complex 2.	38
Figure 27. IR spectrum of complex 2.	40
Figure 28. UV-Vis spectrum of complex 1. Insert: Spectrum of complex 2 in range 460-800 nm.	42
Figure 29. UV-Vis spectrum of cobalt(III) complex 2, black line represents only metal complex signal, and red and green lines show the successive increases in amounts of DNA.	43
Figure 30. Synthesized complex of iron(III) with p-anisaldehyde.	44
Figure 31. a) and b) are proposed structures of complex 3.	44
Figure 32. Octahedral Crystal Field of complex 3.	46
Figure 33. IR spectrum of complex 3.	47
Figure 34. UV-Vis spectrum of complex 3.	48

Figure 35. UV-Vis spectrum of iron(III) complex 3, red line represents only metal complex signal, and green and blue lines show the successive increases in amounts of DNA.....	49
Figure 36. Synthesized complex of iron(III) with cinnamaldehyde.....	50
Figure 37. a) and b) are proposed structures of complex 4.....	50
Figure 38. Octahedral Crystal Field of complex 4.....	51
Figure 39. IR spectrum of complex 4.....	52
Figure 40. UV-Vis spectrum of complex 4.....	53
Figure 41. UV-Vis spectrum of iron(III) complex 4, red line represents only metal complex signal, and green and blue lines show the successive increases in amounts of DNA.....	54
Figure 42. Interaction of ligand based on p-anisaldehyde with 1BNA DNA.....	55
Figure 43. Hydrogen bond from docking with ligand 1.....	56
Figure 44. Interaction of ligand based on cinnamaldehyde with 1BNA sequence.....	57
Figure 45. Hydrogen bond from docking with ligand 2.....	57
Figure 46. Docking of complex 1 with 1BNA. a) Solid Surface of 1BNA with complex, b) Closest atoms of the 1BNA chain with the complex.....	58
Figure 47. Docking of complex 2 with 1BNA. a) Solid Surface of 1BNA with complex, b) Closest atoms of the 1BNA chain with the complex.....	59
Figure 48. Docking of complex 3 with 1BNA. a) Solid Surface of 1BNA with complex, b) Closest atoms of the 1BNA chain with the complex.....	59
Figure 49. Docking of complex 4 with 1BNA. a) Solid Surface of 1BNA with complex, b) Closest atoms of the 1BNA chain with the complex.....	60

LIST OF TABLES

Table 1. Experimental values of complex 1 obtained from magnetic susceptibility balance.	30
Table 2. Experimental values of complex 2 obtained from magnetic susceptibility balance.	37
Table 3. Calculated values of χ_M , χ_{corr} , μ_{eff} from complex 2.	38
Table 4. Possible values to μ_{eff} from complex 2.	39
Table 5. Experimental values of complex 3 obtained from magnetic susceptibility balance.	45
Table 6. Calculated values of χ_M , χ_{corr} , μ_{eff} from complex 3.	45
Table 7. Experimental values of complex 4 obtained from magnetic susceptibility balance.	50
Table 8. Calculated values of χ_M , χ_{corr} , μ_{eff} from complex 4.	51
Table 9. Theoretical value of complex 4.	52
Table 10. Results of docking with autodock of ligand 1.	56
Table 11. Results of docking with autodock of ligand 2.	57

Introduction

Cancer is a disease that involves the uncontrolled growth of cells in a specific part of body.¹ It is a public health problem that has increased in last years, nowadays, cancer has become to a disease of high risk and high impact for all countries due to the increase in deaths, increase of cancer types and the wide range of ages of people who have been affected. The problem of cancer disease is well reflected in GLOBOCAN 2018 report that estimate 18.1 million new cancer cases and 9.6 million cancer deaths in 2018 around 20 region in the world.² Even countries with strong economies and great power, as China³ or United States,⁴ taken this disease like a major public health problem such. Other important fact is the range of ages influenced by cancer, only in 2020 was estimated that 89.500 of adolescent and young adult (15-39 years) were affected in United States, from which 9.270 deaths were estimated.⁵

Although cancer treatment methods have been on the rise, and more cancer survivors have been achieved⁶ since the first indications were made in 1600 BC.¹ Today, the problems associated with these treatments mean that this public health problem remains influential in the world, with the most common types of cancer dominating the world: lung, female breast and colorectal cancers.² Nowadays, treatments such as chemotherapy, surgical extractions or radiotherapy have been used but these still show certain adverse effects in most cases.¹

In 1900, the chemist Paul Ehrlich coined the term “chemotherapy” as the use of chemicals to treat several diseases; in fact, Ehrlich was interested to treat cancer with some drugs such as aniline dyes or the first primitive alkylating agents. One of the first compounds that promoted the research and use of drugs in cancer treatments were the mustard compounds in World War I, in which they obtained encouraging results but not exactly the desired ones. Into 1960s, the surgery and radiotherapy dominated the cancer therapies while cancer treatments with drugs were minimized. However, when surgical extractions or radiotherapy stagnated at an effectiveness of 33%, the search for alternative treatments to improve this value was imperative. For this reason, chemotherapy took on greater importance, in addition to continuing to have the support of many important institutions, medical institutes, organizations and many

scientists, such as the chemotherapist Paul Calabresi who was recognized as the father of this field. Calabresi worked and promoted research and potential uses of chemotherapy, in addition to having the projection that cancer would perish with drugs. This support grew as the positive effects of certain doses of drugs on tumor cells, and the effects on remissions in diseases such as leukemia, were verified. These advances have made it possible to improve radiotherapy treatments, by incorporating chemotherapy, and being able to cure diseases such as Hodgkin's disease in 90% of cases in early stages thanks to this combination. Over time, chemotherapy has evolved and has become "targeted therapy" due to the identifying many molecular targets.⁷

The problems with the mentioned treatments are numerous and diverse such as: the difficult to targeting cancer stem cells, the drug resistance properties of cancer stem cells, lack of cancer epigenetic profiling and specificity of existing epi-drugs, problems associated with cancer diagnosis, unavailability of effective biomarkers for cancer diagnosis and prognosis, limitations of conventional chemotherapeutic agents, metastasis,⁸ and the immediately side effects or late side effects. The "immediately" side effects are problems that affect patients during the treatment such as: vomiting, nausea or several pains,^{9,10} and the late side effects are the problems that the patients could be show after the treatment are finished and even delay some years.^{11,12}

Due to the problems associated with the treatments, remarkable efforts to generate alternatives to reduce the negative effects, and reduce the limitations in such a way that the treatments have a greater effectiveness have been explored. Therefore, several options have been generated such as the use of combined drug,¹³ the combined use of chemotherapy-radiotherapy-immunotherapy,¹⁴ development of new drugs with a more specific target molecule,¹⁵ among many other ways in which cancer treatments can be improved. In this sense, new drugs have been discovered with great potential and promising previous results or that are useful as a starting point. Among those, the cis-diamminedichloroplatinum(II) (cisplatin; discovered in 1845 and used for the first time as anticancer drug in 1960) has great potential against cancer, also helped to understand the importance and effect of geometry and isomerism of metal complexes on the interaction with DNA in cancer cells.¹⁶

With the discovery of the anticancer potentialities of cisplatin, it was the pioneer in this field for metallic compounds, since this field was thought as something exclusive to organic compounds. Cisplatin has a square planar geometry, is neutral and has two labile chloride, which facilitates diffusion through the membranes,¹⁷ also, the characteristics of platinum(II) as a soft Lewis acid conferred it a high affinity to sulfur, and nitrogen donors and lower affinity to oxygen donors, so that platinum in this complex could bind DNA, peptides and proteins through S and N donors.¹⁸ Cisplatin has a mechanism that acts by entering the body and it stays intact in the blood (no loss of chloride ligands is observed). After that, the complex changes chloride ligands to water ligands by the difference between concentration of chloride in the intracellular fluids. This activated complex binds to DNA in N7 position of imidazole ring belong to de guanine or adenine, producing adducts that block replication and cell division.^{19,20}

Due to the remarkable results of cisplatin as anticancer drug, the research on other metallodrugs based on platinum complexes were motivated, and compounds like carboplatin and oxaliplatin was found and investigated to search similar anticancer properties. However, the adverse effects of cisplatin^{16,18} and other platinum-based compounds²¹ associated to the toxicity of platinum in the human body has led to the use of other metals to reduce these effects. Thus, the research about different metals that present interesting characteristics for this purpose become to be popular almost 50 years ago. A clear example of this, are the less exotic metals of group d, which include elements of groups III-XII. Among the most important properties that transition metals show are: charge variation, structure and bonding, metal-ligand interaction, Lewis acid properties, partially filled d shell, and redox activity.²² For this, metals that are essential or present in the body and with properties to promote mechanisms of action that allow attacking various diseases could be used due to their lower toxicity. In this context, transition metals such as iron²³ and cobalt²⁴ that are present in living organisms with relevant functions, could be potential candidates for this purpose. However, not all of these metals prefer to adopt the square planar geometry like cisplatin, in part because square plane geometry is less sterically favored than the tetrahedral geometry and is more prohibitive with long ligands. Even complexes that can be formed as square planar geometry are often turn to octahedral geometry easily. Square planar geometry is

typical of few metals with d^8 configuration such as Ni(II) or Pt(II), and minor frequent for metal ions such as Cu(II), Co(II), or Co(III) with different d configuration.²⁵ In the case of octahedral geometries, the increase of two ligands allow to explore more possible effects associated to this variation as in the case of octahedral Ruthenium complexes²² that have been testing obtaining promising results.

The advances on the synthesis of ligands designed to develop complexes as metallodrugs have allowed to create a category focused on ligands: “the entire inert complex is active, the entire reactive complex is active, a fragment of the complex is active, the metal ion or one of its biotransformation products is active, the metal is a radiation enhancer, the metal is radioactive, and one or more of the ligands is responsible for the biological activity”.²⁶ This allows focusing on the ligands and not just the metals.

A clear example of the importance of the ligands in the development of new drugs, independently the target disease, are the Schiff bases. Complexes containing this type of ligands have shown several biological properties interesting to pharmacological purposes such as: anti-bacterial activity, anti-fungal activity, anti-cancer activity, antioxidant activity, anti-inflammatory activity, and antiviral activity.²⁷

Other important way that could be useful and it has not been so widely used to interact with DNA to produce a reaction in the drugs context, are π - π stacking and other intermolecular interactions. They are mainly non-covalent interactions between aromatic compounds that contain π orbitals. It is due to a lot of possible applications from them and because these interactions can enhance the conformational stability.²⁸ Therefore, there would be greater possibilities of interaction of some aromatic ligands with the DNA chain (Figure 1).²⁹

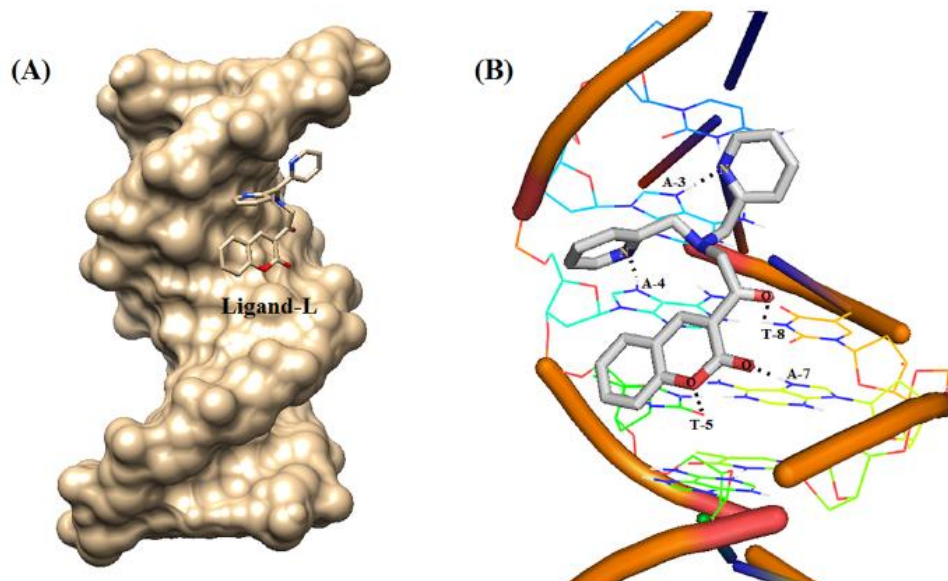


Figure 1. Molecular docked structure of ligand-L complexed with B-DNA. A) Molecular surface view interaction of ligand with DNA. B) Hydrogen bonding interaction of ligand with DNA (PDB ID:1BNA). Taken from Khan.²⁹

Therefore, in the problem statement section will explain that this work is interested in the synthesis of low toxicity metal complexes with the capacity of strong interaction with DNA and related biomolecules.

PROBLEM STATEMENT

Cancer is a public health problem that has been on the rise throughout the world, which has promoted great research efforts to solve it. For this reason, a large number of single and combined treatments against cancer such as chemotherapy have been created, and for this purpose a large number of drugs have been developed. However, many of these drugs show problems such as the so-called side effects or toxicity, so research of mechanism of action, the active principles and the theoretical basis that allows synthesize new friendly and efficient drugs is needed.

To achieve this, is important to synthesize and study new drugs, for example, drugs based on metal complexes, with the potential to attack cancer cells, so they must be able to bind biomolecules as DNA through versatile mechanism. Furthermore, for these studies it is important to have a large amount of theoretical or computational data in order to better understand the behavior of synthesized drugs.

Thus, this work is focused on the synthesis of several metallodrugs based on iron and cobalt complexes containing Schiff bases as ligands, making the complexes as hybrids to interact with DNA either covalent binding (cisplatin mechanism) or through π - π (DNA-ligand) stacking interactions. The general interaction of these complexes with DNA will be evaluated by UV-Vis spectroscopy and corroborate with preliminary docking simulations.

GENERAL AND SPECIFIC OBJECTIVES

General objective

The main objective of this thesis work is to synthesize new metal complexes of cobalt and iron with Schiff base ligands and the evaluation of the interaction of the complexes with DNA.

Specific objectives

In order to reach the main objective of the work, several specific objectives must be completed:

- Extraction of aromatic aldehydes from plants to synthesize Schiff base ligands.
- Synthesize Schiff base ligands through condensation of aldehydes with ethylenediamine.
- Synthesize the iron and cobalt metal complexes with Schiff bases.
- Characterize the complexes using FTIR, magnetic susceptibility, UV-Vis spectroscopy.
- Extraction of DNA from plants.
- Evaluation of the interaction of plant DNA with synthesized complexes.
- Perform theoretical calculations of the interaction between the ligands and obtained complexes with DNA through docking simulations.

CHAPTER 1: Theoretical Framework

1.1. Coordination compounds

A coordination compound, coordination complex or, commonly called complex, is the product of the formation of covalent coordination bonds. The coordinated bond is based on the donation of a pair of electrons of an orbital in an atom that will occupy an empty orbital in another atom, this pair of electrons of the bond originates only in one of the two associated atoms, here an electron pair acceptor and electron pair donor.

In many cases, in coordination compounds a central atom or ion is linked to several other atoms, ions or groups through a coordinated bond and not just to one of these at once. The central atom, which is a metal or metalloid, is an electron pair acceptor, and the species around it must have at least one lone pair of electrons to donate to an empty orbital in the central atom, these donor species joining forming the binding are called ligands.

The ligands are of variable sizes, small like a monatomic ion or large like a polymer, but they must have one or more pairs of lone electrons in an electronegative donor atom, among the most common atoms donors are heteroatoms like N, O, S and P. However, many of the existing organic molecules can act as ligands, or can be converted to ligands, depending on their ability to give a pair of electrons.³⁰

1.2. Medicinal coordination compounds

The use of coordination compounds as drugs has been increasing in last years; pharmaceutical preparations formulated to treat specific diseases of essential metal management problems *in vivo* have been used commonly. For example, copper complexes are used in Menkes disease in which there is a deficiency of copper due to a defect in the intracellular transport of this metal. Since the administration of copper salts was ineffective and with the knowledge that exchangeable copper in human blood serum involves complexes of copper-histidine that bind to serum albumin, it was possible to use copper histidine coordination compounds in the treatment of this disease, obtaining results such as suppressing the neurodegeneration that arises from Menkes disease if it is applied early. Another interesting application is the case of

chelation therapy in which selective complexing agents can be used to sequester unwanted metals *in vivo* and eliminate the body by excretion.³¹

Interestingly, in recent years there has been a greater impact on the use of metal complex drugs with some anticancer effects, this is reflected in world economy since it was estimated that one billion dollars was involved in platinum anticancer drugs market in the 2000s. The use of coordination compounds in medicine has been greatly promoted since the discovery of the anti-cancer activity of *cis*-[Pt(NH₃)₂Cl₂] in 1960 when Rosenberg, Van Camp and Krigas demonstrated that this complex could suppress cell division giving place to the clinical use of the drug cisplatin.³¹ In addition, this allowed to understand the effect of geometry and isomerism of anticancer complexes in cancer cells and how they interact.¹⁶ Therefore, several attempts have been made in order to understand the mechanism of action of cisplatin and to trying to develop new drugs with reduced side effects and increased anticancer activity. Regarding drugs based on the medicinal properties of platinum compounds, drugs such as carboplatin, nedaplatin, or oxaliplatin were also tested.³¹

In addition to the known platinum compounds, anticancer potentialities have also been found in other metal ions such as zinc(II), copper(II), gold, and copper chelating agents, ruthenium-containing compounds,³² iron,²³ or cobalt.^{24,33,34}

1.3. Schiff bases ligands

Schiff bases contain C=N bond in their structure, it can be referred to imine or azomethine functional group, commonly the synthesis of Schiff bases is carried out by the condensation of amines with aldehydes or ketones where the C=O group is replaced (Figure 2). Ligands based on Schiff bases are easily coordinate to metal, and they have interest biological applications such as antifungal, antiviral, antibacterial, anticancer, antioxidant and anti-inflammatory, also like a catalyst in several reactions such as reduction reaction of ketones, Diels-Alder reaction, Henry reaction, among others.²⁷

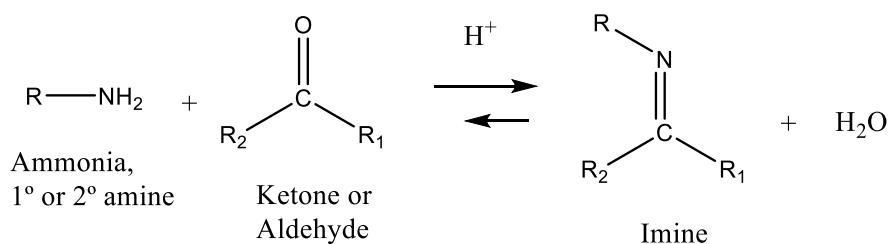


Figure 2. Scheme of Schiff base condensation mechanism from amines.

1.4. Cobalt complexes

Cobalt is an essential element for animals due to the biological roles of which it is a part. For example, a cobalt metal center is in vitamin B12 (cobalamin), in this case, the metal is found as cobalt(I) but it can change to cobalt(II) or cobalt(III). The importance of cobalamin lies in the formation of red blood cells, maintenance of the brain and its nervous functions in addition to synthesis and regulation of DNA, so cobalt may be less toxic to humans than non-essential metals in the human body. Based on this fact, a large number of cobalt drugs have been synthesized and tested for different purposes, for example, Doxovir that is an experimental drug of Co(III)-complex that has potential antiviral effects for Herpes labialis.²⁴

Due to these biological potentialities, metal drugs that can act as anticancer agents have also been synthesized and tested. In this sense, cobalt compounds such as some hexacarbonyl dicobalt complexes have been tested due to their potential in breast cancer cell line. In the same way, it was discovered that cobalt-alkyne complexes could inhibit cyclooxygenase, which can delay tumor growth and enhance response to other therapies. Other cobalt complexes interact with nucleoside ligands showing antiproliferative activity with IC_{50} around 5-50 mM in human breast cancer.^{33,35} Schiff bases have also been used as coordinating ligands in cobalt complexes and promising results of its anticancer activity (against human breast cancer cells) have been reported, for example, a complex of cobalt(III) with tridentate Schiff base ligands from salicylaldehyde and ethylenediamine was reported with $IC_{50} < 100 \mu\text{M}$.³⁴

1.5. Iron complexes

Iron is an essential element for mammals due to the biological roles of which it is part, such as erythropoiesis, electron transport, or DNA synthesis.²³ In addition, due to the

increase in the search for new drugs based on metals with promising potentialities in several diseases, iron has been one of the metals in which their research has increased.

The tests carried out on several complexes of iron coordinated with *salen*-like (*salen* = N,N'-Ethylenebis(salicylimine)) ligands studied by Ghanbari,³⁶ show potentiality against cancer with values of PIC₅₀ (log IC₅₀) close to that of cisplatin, although the geometry and nature of the substituents present in the ligand could control the cytotoxicity profile.

Other iron complexes with *salen*-like ligands synthesized from camphoric acid showed IC₅₀ values between 11 and 27 μM against cell lines of breast, melanoma, and colorectal cancer.³⁷

1.6. Mechanism of action from metal-based drugs

The mechanism of action allows to understand how work the metal-based drugs, these can be classified into: covalent binding of metal-based drugs to biomolecules, inhibition of enzymes via substrate and metabolite mimics, redox-active drugs, photoactivatable compounds for photodynamic therapy and photoactivated chemotherapy, metal complexes for delivery and release of pharmacologically active ligands, catalytic drugs, radio-imaging and therapy with radio-metals and radioactive agents, MRI contrast agents, and other miscellaneous modes of action.

1.6.1 Covalent binding of metal-based drugs to biomolecules

This mechanism of interaction is carried out by covalently bonds between metal ion (usually with labile ligands) and essential biomolecules such as DNA, this inhibits their functions and leading to cellular pathways of cell death. This method is used by cisplatin¹⁹ which is a compound that has a square planar geometry, is neutral and has two labile groups (Cl⁻) to facilitate diffusion through membranes.¹⁷ Platinum shows a behavior of as a soft Lewis acid having a high affinity for sulfur, and nitrogen donors and lower affinity to oxygen donors, so platinum in this complex could bind DNA, peptides and proteins through S and N donors.¹⁸ The anticancer activity of this compound is due to the antitumor properties that it shows through binding to DNA and due to the formation of specific adducts, thus inhibiting DNA replication. To initiate the mechanism

of action, cisplatin must remain intact in the extracellular fluids, which is possible due to the relatively high concentration of chloride, to later allow the exchange of these chloride substituents in the intracellular ones. The reactivity of the latter and their characteristic of better leaving groups allow the reaction with cellular nucleophiles such DNA (Figure 3).

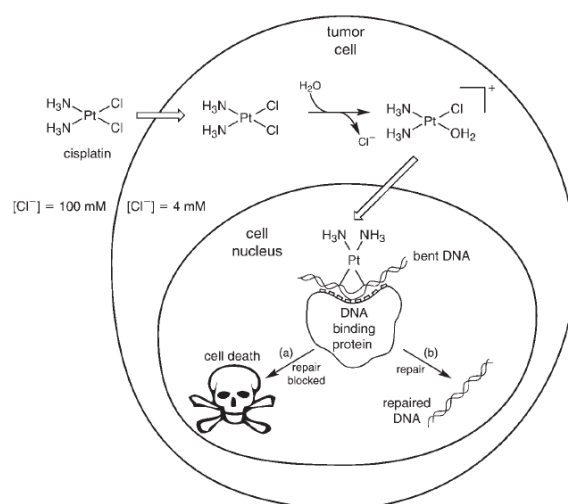


Figure 3. Scheme of mechanism of binding between DNA and cisplatin, taken from Alderden.¹⁶

Studies on this mechanism have led to know that cisplatin tends to react more commonly with the N7 position of imidazole ring belong to de guanine or adenine with which it forms monofunctional or bifunctional adducts. Between the main adducts belong to cisplatin are: GpG 1,2-intrastrand (the most common), that consists of binding to adjacent deoxyguanosines in the same strand of DNA. Other important adducts but less common are the ApG 1,2-intrastrand, finally in a lower proportion are the GpXpG and ApXpG 1,3-intrastrand, monofunctional intrastrand, and interstrand crosslinks (G-G) (Figure 4), these adducts are those that block replication, also, they are responsible for prevent transcription.²⁰

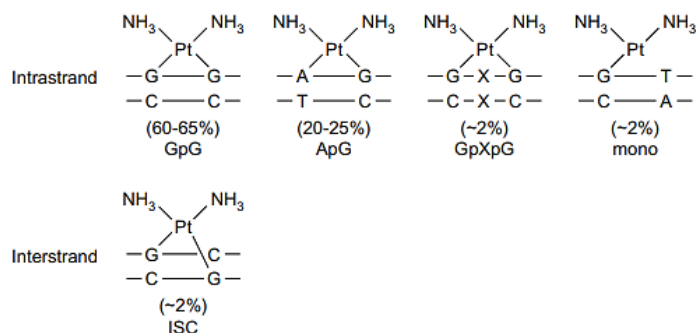


Figure 4. Major types of cisplatin adducts produced by binding of cisplatin with DNA taken from Kelland.²⁰

1.7. π - π stacking interactions

The π - π stacking interactions are non-covalent interactions between moieties of aromatic compounds containing π orbitals. This type of interactions is non-destructive and reversible. The large number of compounds of this type gives a wide range of possible applications from controlled drug release, design of molecular receptors or DNA sequencing among other biological applications. Furthermore, these interactions can be considered as conformational stability enhancers.²⁸

Studies of the geometric factors of these interactions suggest that parallel displaced and T-shaped conformations are the most stable (energy minima), and sandwich (face to face) configuration is unstable because the overlap of the π system is maximized.²⁸ Some interactions like Van der Waals or electrostatic have been discussed to stabilization of π - π interactions on closed shell molecules, like: dipole-dipole, dipole-induced dipole or induced dipole-induced dipole that are attractive interactions. However, π interactions can be affected by Pauli repulsion by very short distances between filled electron clouds, solvophobic effects when polar solvents carry to desolvation and this stabilize the aggregation of lipophilic molecular surfaces, or charge transfer that can be referred to a stabilization.³⁸ The interactions of π - π stacking can occur in two aromatic molecules with similar electron distribution structures, and also in molecules rich in electrons and deficient in electrons but with dependence on the polarity of the solvent. Also, the aromatic π clouds apparently show some facility for delocalized, which means better intermolecular electrostatic interactions than nonaromatic molecules.²⁸ Figure 5 shows the main orientations of aromatic-aromatic interactions.

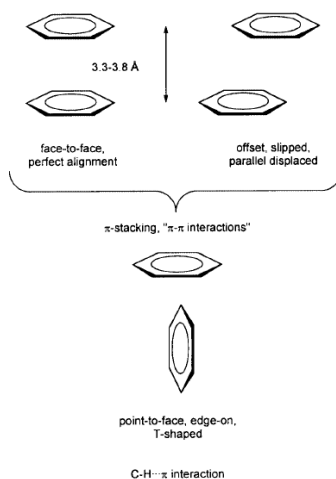


Figure 5. Main orientations of aromatic-aromatic interactions taken from Janiak.³⁸

1.8. Electronic states in Metal Complexes

The electronic structure associated to complexes can be studied through the tools like UV-Vis spectroscopy. Different electronic transitions could be differentiated through their energy (wavelength) and their probability (molar absorptivity coefficient, ϵ) depending on the nature of such transition,³⁹⁻⁴¹ the next sections describe a series of electronic transitions and their origin.

1.8.1. Metal Centred (MC) or d-d transitions

These transitions involve electron transitions between d orbitals of transition metals, they are Laporte forbidden, and could be Spin forbidden depending on the ground state of the metal. These transitions are weak ($\epsilon \approx 1 \cdot 10^{-2}$ L/mol·cm), and could be masked by other transitions.⁴⁰

1.8.2. Charge transference (CT) or optical electron transfer transitions

This type of transition commonly has $\epsilon \approx 10^2$ - 10^6 L/mol·cm and are divided in three groups: metal-to-ligand charge transfer (MLCT), ligand-to-metal charge transfer (LMCT), and charge transfer to solvent (CTTS). The CT excited states commonly lead to redox reaction, and this is referred to transfer of electronic charge from a region of molecule to other.³⁹ MLCT moves an electron from orbitals with metal character to orbitals with ligand character, and it is associated with the lower energy of charge transfer transition by the low energy of π acceptor orbitals typically found in ligands from organometallic

complexes.⁴¹ Bands associated to LMCT transitions are commonly visible to UV region, in this case the electrons are transferred from orbitals with ligand character to orbitals with metal character.

1.8.3. Ligand centered (LC) or intra-ligand transitions

These are transitions between molecular orbitals localized on the ligand system, the bands associated are found at relative low energies in complexes with π systems, some aromatic ligands belong to this transition. This transitions are clearly identified when the fixed spectral position is independent of oxidizing character of central metal.³⁹

1.9. DNA concentration and purity

The use of UV-Vis spectrophotometry has been widely used to detect characteristic signals from biomolecules, it is useful to determine the purity and quality of nucleic acids like DNA. In order to measure the DNA concentration (N), the equation 1 is used.

$$N = \frac{A_{260}}{\epsilon_{260}} \quad (1)$$

Where A_{260} is the absorbance at 260 nm and ϵ_{260} is the corresponding DNA molar absorptivity coefficient at this wavelength. The use of A_{260} is due to the presence of maximum absorbance at 260 nm and minimum at 234 nm of DNA, however, these values can be affected by many factors like pH of medium, DNA degradation, or hydrodynamic shearing, among others.

The most used parameter to measure the purity of DNA extracted is through $A_{260}:A_{280}$ ratio, because the concentration of proteins shows maximal absorption at 280 nm, due to the presence of tryptophan, tyrosine and phenylalanine. Values in the range of 1.8-2.0 are characteristics of pure DNA, 1.6-2.0 range is taken as sufficiently pure, values above 2.0 show the presence of RNA, and values below 1.8 show the presence of protein.⁴²

1.9.1. DNA-drug interactions measurements

The interactions produced by the binding of ligand molecules (drugs) and nucleic acids produce optical changes that can be detected by optical absorbance technique, and it

can be used for the calculation of binding constant to obtain information about the nature or strength of the DNA-ligand interactions.

The expected behavior to successful interaction are: bathochromic effect (increase of wavelength) and hypochromic effect (decrease of molar extinction coefficient), however, these effects does not show the specific binding mode (groove binding, DNA intercalation or effect of another drug).⁴³

If the ligands have aromaticity, the interaction with DNA is through intercalation, which increases the axial length of these as it separates the base pairs. The intercalation allows the π - π stacking interaction a produce a hypochromic effect in the absorbance of DNA if aromatic ligands can interact with the base pairs of this, the measure of shift is associate to binding strength. This can measure with the equation 2,

$$\frac{[DNA]}{(\varepsilon_a - \varepsilon_f)} = \frac{[DNA]}{(\varepsilon_b - \varepsilon_f)} - \frac{1}{K_b} (\varepsilon_b - \varepsilon_f) \quad (2)$$

Where, K_b is the binding constant, ε_b is extinction coefficient of the metal complex, ε_f is the extinction coefficient of the free complex, and ε_a is the apparent absorption coefficient of the complex.⁴⁴

1.10. Docking Simulations

The use of computational methods related to medicinal chemistry have been increasing in the last years and is reflected by the increase in papers associated to this, due the enhancement of software associated and the importance of information that can give us to understand and explain the activity of compounds or even to filter good candidates from hundreds of ligands for future research. In this sense, the molecular docking is computational method used to predict the interaction between two molecules, examples of these binding are small molecule-macromolecule (protein-ligand), or binding between two macromolecules (protein-protein).

The molecular mechanics, base of most docking programs, describes the polyatomic systems with classical physics. Here, parameters like charges, torsional and geometrical angles are taken account to approximate the computational method to experimental

data. In this sense, the forcefield are used to describe the systems too, examples of these forcefield are AMBER, GROMOS, MMFF94, CHARMM, and UFF.⁴⁵

1.10.1 Autodock software

Autodock 4 is a tool of automated docking that combines an empirical free energy force field with a Lamarckian Genetic Algorithm that allow the prediction of bound conformations and binding energies of proposed ligands with macromolecules. Autodock uses a grid-based method, this to measure the binding energy of conformations, here, the probe atoms are tested in each grid point where the target protein is located, and these values are saved in the grid. In the docking the values of grid are used to the search minimums with ligand interactions.⁴⁶

1.10.2 Hex 8.0.0 software

Hex 8.0.0 is a tool originally used for protein-protein docking, however in recent years it was tried to perform docking between metal complexes and DNA. This software uses spherical polar Fourier correlations instead of search based on the Fast Fourier Transform. It is due the rotational and translational degree of freedom used that produces a reduction on execution time. Hex uses dense sampling of the search space, after this it groups the solution with a similar orientation.⁴⁷ In the last years, the use of Hex software has focused to predict interactions that provide information for the design of several drugs.⁴⁸

CHAPTER 2: Methodology

2.1. Reagents

Ethylenediamine ($C_2H_8N_2$) $\geq 99.5\%$, Sigma-Aldrich.

p-anisaldehyde ($CH_3OC_6H_4CHO$) 98%, Sigma-Aldrich.

Chloroform ($CHCl_3$) $\geq 99.0\%$, ISOLAB chemicals.

Magnesium sulfate ($MgSO_4$).

Potassium chloride (KCl).

Sodium chloride (NaCl).

Di-Sodium hydrogen phosphate (Na_2HPO_4) 99%, lobachemie.

Potassium dihydrogen phosphate (KH_2PO_4) 99.6%, Fisher Scientific.

Hydrochloric acid (HCl) 36.5-38%, fisher chemical.

Iron (III) nitrate nonahydrate ($Fe(NO_3)_3 \cdot 9H_2O$) $\geq 98\%$, Acros, ThermoFisher Scientific.

Cobalt (II) chloride hexahydrate ($CoCl_2 \cdot 6H_2O$) 98%, Sigma-Aldrich

Methanol (CH_3OH) 99.8%, fisher chemical.

Dimethyl sulfoxide (DMSO) $\geq 99.9\%$, Sigma-Aldrich.

Glacial acetic acid (CH_3COOH) 100%, Merck.

Sodium tetrphenylborate ($(C_6H_5)_4BNa$) $> 99.5\%$, Sigma-Aldrich.

Sodium bicarbonate ($NaHCO_3$)

Acetonitrile (C_2H_3N) $> 99.9\%$, fisher chemical.

Hexane (C₆H₁₄) ≥98.5%, fisher chemical.

Ethyl acetate (C₄H₈O₂) ≥99.5%, fisher chemical.

2.2. Laboratory Equipment

Cary 630 FTIR Spectrometer, Agilent Technologies.

MK1 Magnetic Susceptibility Balance, Sherwood Scientific Ltd.

LAMBDA 1050+ UV/Vis/NIR Spectrophotometer, PerkinElmer.

Rotary evaporator R-210, BUCHI.

2.3. Cinnamaldehyde extraction

The procedure used to extract this aldehyde was a simple distillation system according to literature.⁴⁹ The cinnamon barks were broken in small pieces, a quantity of these (60 g) were placed in round bottom flask with 200 mL of distilled water, and this flask was placed to simple distillation system. After 2 hours, with temperature control that allowed the emergence of a distilled, the cloudy white liquid obtained is collected. This liquid was washed with 30 mL of chloroform, and the obtained phases were separated and collected from separatory funnel. MgSO₄ was added to the phase with cinnamaldehyde, then, was filtered to separate the liquid, and finally the product was placed in rotary evaporator to quit chloroform.

2.4. Synthesis of Ligands

The applied procedure for the synthesis of Schiff base ligands was the commonly used in the condensation of aldehydes with amines.^{50,51} The two ligands were prepared using a reflux system for about 8 hours, the condensation of *p*-anisaldehyde or cinnamaldehyde with ethylenediamine was carried out in 30 mL of methanol in a 2:1 molar ratio. Here, were used 1 mL of *p*-anisaldehyde with 0.275 mL of ethylenediamine for ligand 1, and 1 mL of cinnamaldehyde with 0.2655 mL of ethylenediamine for ligand 2. A few drops of glacial acetic acid were necessary to achieve a pH of 5 to 6 to make condensation possible.

2.5. Synthesis of $[\text{Fe}(\text{DMSO})_6](\text{NO}_3)_3$

This complex was prepared following the procedure reported in literature,⁵² in the synthesis was used 3 g of $\text{Fe}(\text{NO}_3)_3 \cdot 9\text{H}_2\text{O}$ with 50 mL of DMSO using a reflux system under constant stirring and heating conditions by 2 hours. After that, a green-yellow precipitate was obtained, which was filtered at vacuum and stored in a desiccator.

2.6. Synthesis of Complexes

To obtain the novel complexes was necessary the addition of a salt with the desired metal to coordinate with the ligands. Four complexes were prepared, from which two complexes were obtained cobalt and two complexes with iron.

2.6.1. Synthesis of the Cobalt (III) complex with the ligand derivate from *p*-anisaldehyde.

This complex was prepared with a 30 mL solution of ligand 1 and 0.9787 g of $\text{CoCl}_2 \cdot 6\text{H}_2\text{O}$ in a molar ratio 1:1 in methanol, this process was carried out under reflux conditions for 12 hours under constant stirring and heating around 60 °C.

2.6.2. Synthesis of the Cobalt (III) complex with the ligand derivate from cinnamaldehyde.

This complex was prepared with a 30 mL solution of ligand 2 and 0.9449 g of $\text{CoCl}_2 \cdot 6\text{H}_2\text{O}$ with molar ratio 1:1 in methanol, this process was carried out under reflux conditions for 12 hours under constant stirring and heating around 60 °C. Additionally, in this complex some drops of a cold saturated solution of sodium tetraphenylborate in methanol was necessary to precipitate the product.

2.6.3. Synthesis of the Iron (III) complex with the ligand derivate from *p*-anisaldehyde.

This complex was prepared with a 30 mL solution of ligand 1 and 2.9232 g of $[\text{Fe}(\text{DMSO})_6](\text{NO}_3)_3$ with molar ratio 1:1 in methanol, this process was carried out under reflux conditions for 12 hours under constant stirring and heating around 60 °C.

2.6.4. Synthesis of the Iron (III) complex with the ligand derivate from cinnamaldehyde.

This complex was prepared with a 30 mL solution of ligand 2 and 2.8222 g of $[\text{Fe}(\text{DMSO})_6](\text{NO}_3)_3$ with molar ratio 1:1 in methanol, this process was carried out under reflux conditions for 12 hours under constant stirring and heating around 60 °C.

2.7. Phosphate-buffered saline (PBS) preparation

This preparation was carried out with a common procedure, 80 mL of distilled water are placed in beaker and the next components was successively added: 800 mg NaCl, 20 mg KCl, 144 mg Na_2HPO_4 , 25 mg KH_2PO_4 . After that, the pH was adjusted with HCl and top up with 20 mL of distilled water.

2.8. Vegetable DNA extraction

The applied procedure was similar to the used in literature about vegetable DNA extraction.⁵³ First, the lysis solution was prepared with 125 mL of cold distilled water, one spoon of salt, three spoons of sodium bicarbonate, and two spoons of dish soap, this solution should keep on ice. A banana was crushed with the 25mL of cold distilled water, then, 10 mL of last preparation was mixed with a 20 mL of lysis solution. Then, the mixture was shaken by two minutes and set in ice bath until disappear the half of foam, this mixture was filtered to separate tissue strains of molecular broth. Finally, in 10 mL of the last solution in test tube was added 10 mL of cold ethanol, the white filaments at the water-alcohol interface were collected in PBS.

2.9. DNA interaction with complexes

In order to evaluate the interaction of the complexes with DNA, PBS (with a pH of 7) was added to a DNA collected and it was sonicated for 25 cycles, 30 seconds with intervals of 1 minute between the cycles.⁵⁰ The solution of PBS with DNA was mixed in different quantities with the four complexes in independent experiments, then the mixture were placed in a solution of DMSO (around 0.5%) with water/acetonitrile and measured with UV/Vis Spectrophotometer.

2.10. Characterization techniques

2.10.1. Infrared Spectroscopy (IR)

Infrared spectra were determined in a Cary 630 FTIR Spectrometer in the range of 400-4000 cm^{-1} . IR was used to characterize the cinnamaldehyde and the four synthesized complexes. Both liquid and solid samples were measured.

2.10.2. UV-Vis Spectroscopy

Electronic absorption spectra were determined in a LAMBDA 1050+ UV/Vis/NIR Spectrophotometer in the range of 200-800 nm for both solutions of the free complexes and solutions of DNA in PBS. Measurements were performed in 3 cm^3 quartz cuvettes.

2.10.3. Magnetic Susceptibility

Magnetic Susceptibility was determined in a MK1 Magnetic Susceptibility Balance. The first step was to put on zero the balance, such step looks obvious but this type of balance has an analogic system of buttons and due to se sensitivity of the platinum wire inside the box, stabilization of the balance in zero value is a little difficult. In the next step a tube was measured with a standard sample to determine the constant (**C**) of the balance using the equation 3:

$$C = \frac{S_{theoretical} - S_{real}}{S_{theoretical}} \quad (3)$$

Then, it proceeds to weigh the tubes to be used (m_o) and measure the empty tube in the magnetic balance (R_o). After that, the samples were packed carefully, the filled tube was weighed (m) and the height (L) of the compound in the tube was measured to finally measure the tube with the sample (R) on the balance. With the experimental data obtained, the mass susceptibility (χ_g) was obtained through the equation 4:

$$\chi_g = \frac{CL(R - R_o)}{10^9(m - m_o)} \quad (4)$$

2.11. Docking studies of ligands-DNA with Autodock4

In order to perform the docking studies, as a preliminary approach to determine the interaction of our complexes with DNA, it is proved only the free Schiff-base ligands

against the DNA sequence with PDB:1BNA. These preliminary studies allow us to have a good idea about π - π stacking interactions of our complex in the next simulations. For this purpose, Auto grid must be run to generate pre-grid maps for 1BNA which is the receptor. The pre-grid is prepared removing waters, merge non-polar hydrogen, and adding Gasteiger charges to macromolecule and ligands.

The next steps are to prepare the grid parameters on the macromolecule (PDB:1BNA) and choose each synthesized ligand, then define the Grid box, and save the GPF output file. Finally, the Autogrid tool runs.

Finally, the parameters to docking are chosen like set rigid file (macromolecule), choose each synthesized ligand, select the search parameter, and save the DPF output file. In order to have graphical results to the interaction, the Autodock tool run was used.

2.12. Docking studies of complexes-DNA interactions with Hex 8.0.0 software

In the docking of the complexes with DNA (PDB ID:1BNA), all water molecules were removed from 1BNA. In this procedure were used the optimized complexes in PDB format and 1BNA. To run the docking, these molecules were load as Ligand and Receptor respectively. After, the parameters of correlation type must be adjusted as "shape only" in the software.

CHAPTER 3: Results and discussion

3.1. Cinnamaldehyde extraction

The extraction of cinnamaldehyde from cinnamon barks was carried out through simple distillation system (Figure 6), this procedure was detailed in the previous section. The obtained product was a yellow liquid with strong odor (Figure 7), and the extraction process had a 4.03% yield. The presence of this aldehyde is supported by many studies,⁵⁴ also the information obtained from infrared spectroscopy in the next section confirm the characteristics bands of this aldehyde.



Figure 6. Simple distillation system used in the extraction of cinnamaldehyde.

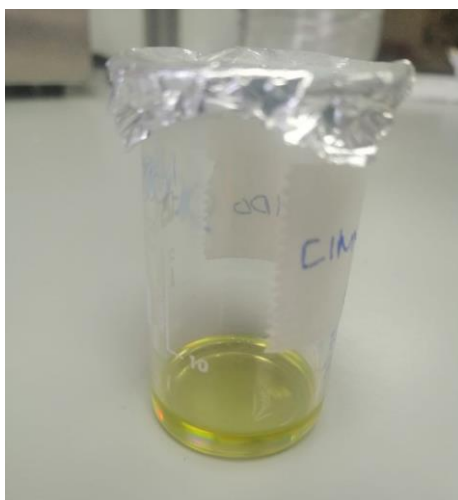


Figure 7. Cinnamaldehyde obtained.

3.1.1. Infrared spectroscopy of Cinnamaldehyde

The product obtained is a yellow oil that show the characteristics bands of aldehydes.⁵⁵ The Figure 8 shows a band between 1680-1675 cm^{-1} that corresponds to C=O of aldehyde affected by longer conjugated system. A band around 2815 cm^{-1} and 2740 cm^{-1} is assigned to C-H band, 1626-1622 cm^{-1} band and around 1450 cm^{-1} that correspond to C=C in aromatic rings, 3020 cm^{-1} sp^2 C-H stretch, and the out of plane bending around 747 cm^{-1} and 687 cm^{-1} bands to correspond monosubstituted ring. These bands confirm the presence of aldehyde, the aromaticity ring, even the mono substitution of this organic molecule, this experimental data collected suggest to presence of the required aldehyde.

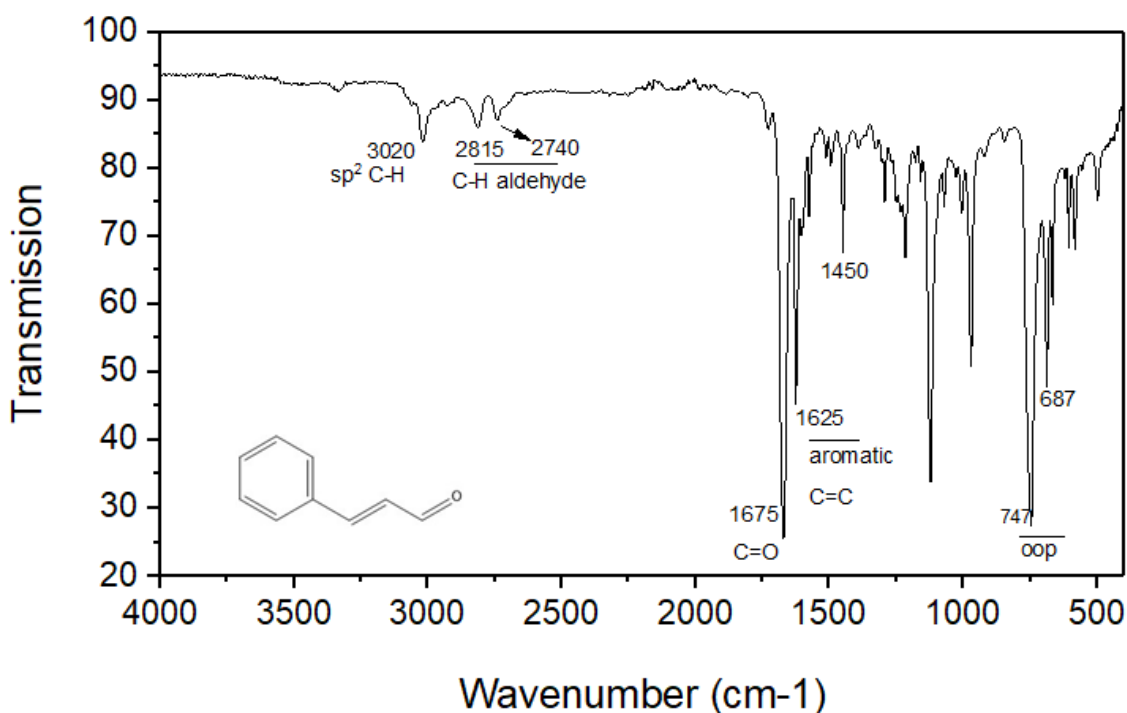


Figure 8. IR spectrum of the extracted cinnamaldehyde.

3.2. Synthesis of Ligands

The procedure used to synthesize the ligands was through a reductive amination both for cinnamaldehyde or *p*-anisaldehyde with ethylenediamine. The mechanism of ligand formation is showed in Figure 9.

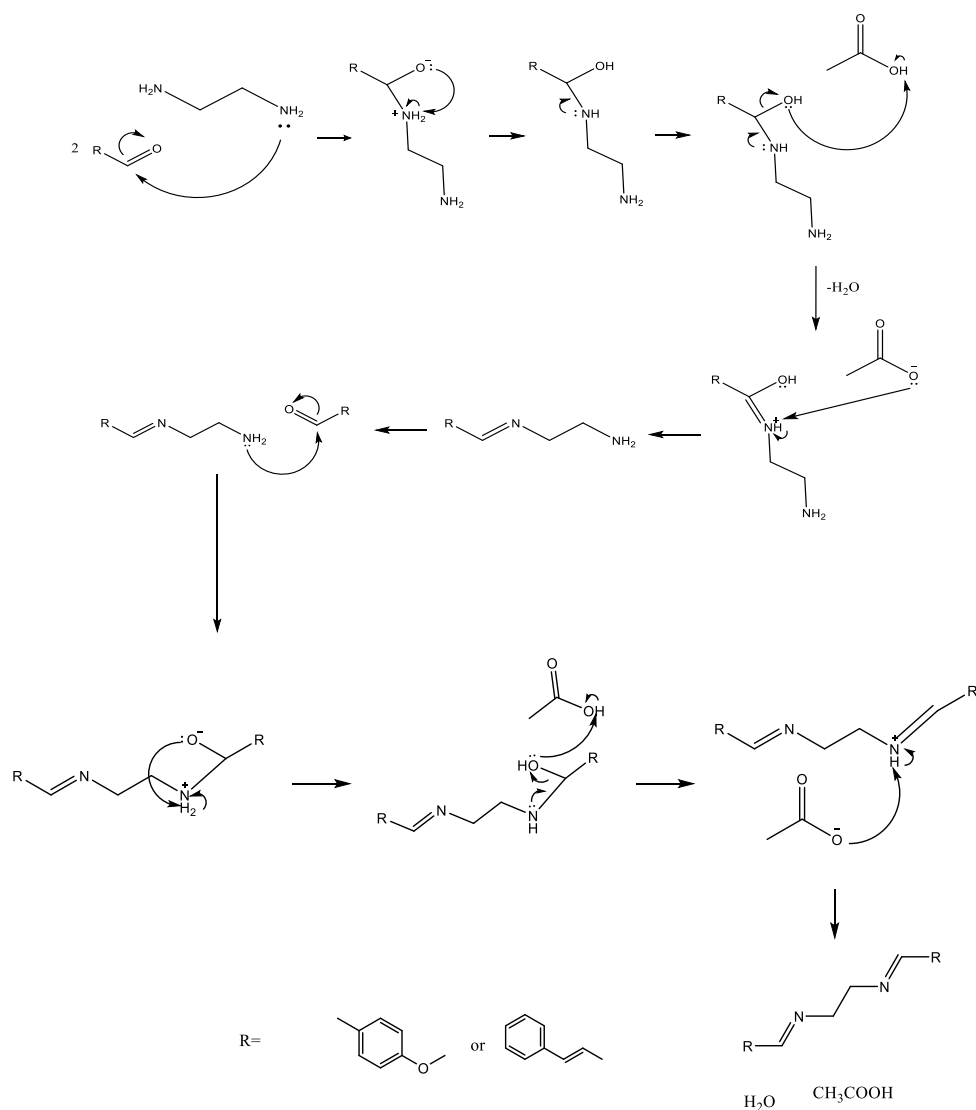


Figure 9. Mechanism of formation of proposed ligands.

In order to synthesize ligands with high content of π -orbitals, it was used a 2:1 molar ratio to aldehyde and amine respectively. An important step to carry out the reaction is the addition of acid because it allows the formation of acidic medium that is necessary to imine formation, thus, pH is a key parameter in this reaction. When decreasing pH from 10 to 6~5, it is clearly the advance of the reaction by the changes in color from light yellow to intense yellow until brown (Figure 10), typical of imines.

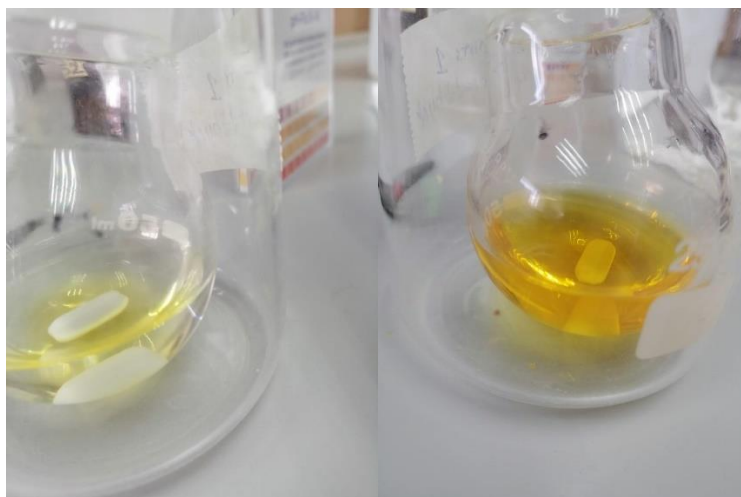


Figure 10. Change of color after addition of acid.

These reactions were followed by TLC (Thin Layer Chromatography), taking advantage of the presence of aldehydes in reactions. Both reactions were followed comparing the spot of the aldehyde reactant with the reaction mixture containing aldehyde and amine. TLC plates were used with a mobile phase of hexane:ethyl acetate in ratio 7:3, and revealed with iodine chamber. In Figure 11 shows the reaction corresponding to the synthesis of the ligand based on *p*-anisaldehyde (ligand 1). Only *p*-anisaldehyde spot is observed throughout the reaction in TLC plate with $R_f = 0.44$, and the spot of ligand disappear after the time mentioned (Figure 12).

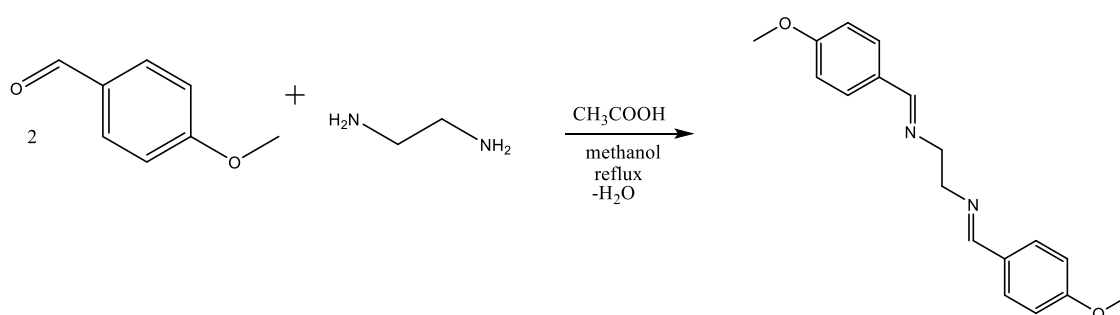


Figure 11. Scheme of reaction between *p*-anisaldehyde with ethylenediamine.

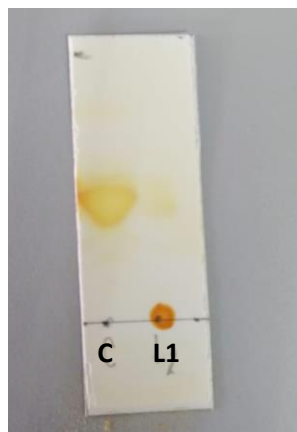


Figure 12. TLC plate of only *p*-anisaldehyde (C), and the ligand based on *p*-anisaldehyde (L1).

On the other hand, in Figure 13 shows the reaction corresponding to the synthesis of the ligand based on Cinnamaldehyde (ligand 2). As in the case of ligand 1, only cinnamaldehyde spot is observed clearly ($R_f = 0.48$), and at difference to ligand 1, the spot of ligand does not disappear completely at all after the time mentioned (Figure 14). The spots showed in the last TLC plate could be by the presence of impurities in the aldehyde.

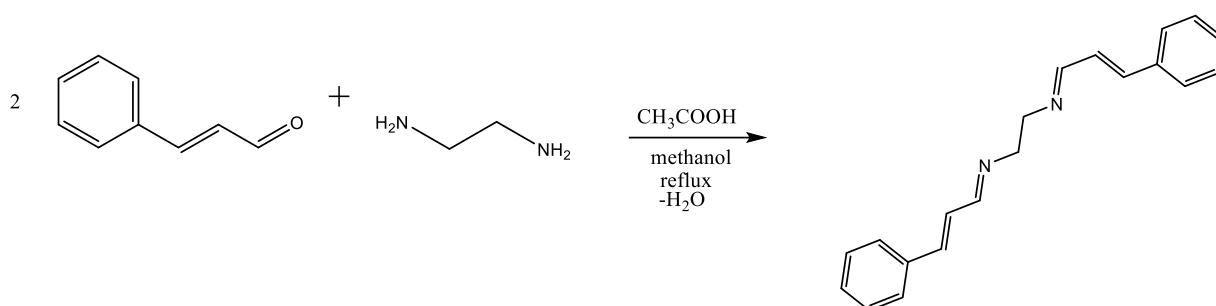


Figure 13. Scheme of reaction between cinnamaldehyde with ethylenediamine.

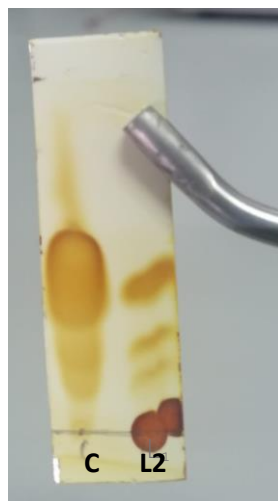


Figure 14. TLC plate of only cinnamaldehyde (C), and the ligand based on cinnamaldehyde (L1).

3.3. Cobalt complex with ligand based on *p*-anisaldehyde (complex 1).

This synthesized cobalt complex was obtained through of procedure detailed in previous section. The precipitation of this complex took around 12 hours under reflux conditions, and the complex was obtained after a vacuum filtration with methanol. The obtained product was a powder very light pink nearly white color (Figure 15).



Figure 15. Synthesized complex of cobalt(III) with *p*-anisaldehyde.

The possibilities of coordination between the metal and ligands are showed in the Figure 16. Both possibilities have octahedral geometry, and it is argued by the experimental results that will be presented in next sections.

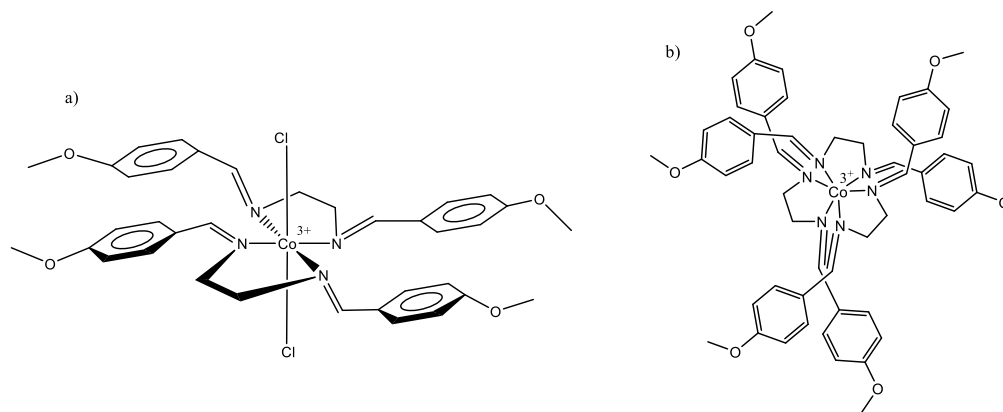


Figure 16. a) and b) are proposed structures of Complex 1.

3.3.1 Characterization of complex 1 by magnetic susceptibility.

An important parameter to characterize the complex is the magnetic moment, and to obtain this value, magnetic susceptibility was determined. The experimental values to calculate the value of magnetic susceptibility per gram were measured at room temperature, and the obtained values are showed in Table 1.

Table 1. Experimental values of complex 1 obtained from magnetic susceptibility balance.

	m_{empty} (g)	m_{full} (g)	R_o	R	L (cm)	C
Complex 1	0.8335	0.9299	-35	-66	2	0.97

The value of C is calculated with the equation 3, previously mentioned, it is useful to calculate the magnetic susceptibility per gram. The experimental value of χ_g obtained with the equation 4 was: $-6.2386 \times 10^{-7} \text{ g}^{-1}$, this negative value is unambiguously assigned to a diamagnetic compound, hence an analysis or calculation of μ_{eff} are unnecessary, so, the only one option for the complex, is the presence of a cobalt(III) with $[\text{Ar}]3d^6$ Low Spin configuration.

3.3.2. Crystal Field Theory of complex 1.

With the supporting of Crystal Field Theory (Figure 17), the theoretical values of μ_{eff} can be calculated using the equation 5,

$$\mu_{eff} = 2\sqrt{S(S + 1)} \quad (5)$$

Where S is the number of unpaired electrons divided by two, however the value of μ_{eff} to cobalt(III) is not calculated because it has not unpaired electrons and means that is diamagnetic substance.⁵⁶

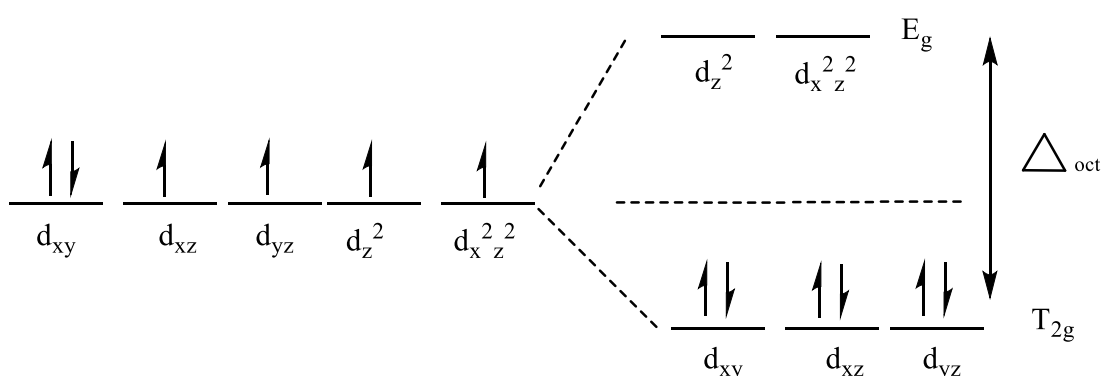
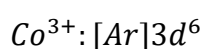


Figure 17. Octahedral Crystal Field of complex 1.

According to the equation 5, is not possible to calculate values of μ_{eff} to metals without unpaired electrons, all these facts support that the metal species was oxidized from cobalt(II) to cobalt (III). Therefore, the question of what reaction is responsible of the oxidation of cobalt emerges.

A rationalized explanation to such cobalt oxidation is: The initial reactant hexaaqua-cobalt(II) complex has a high redox potential ($E = 1.83$ V/NHE), so, oxygen ($E = 1.44$ V/NHE) from air is unable to oxidize this cobalt, however, when the coordination sphere of cobalt changes (specially with nitrogen donor ligands as Schiff bases), the redox potential can be tuned to lower values ($E \approx 0.11$ V/NHE) thus allowing the oxidation of

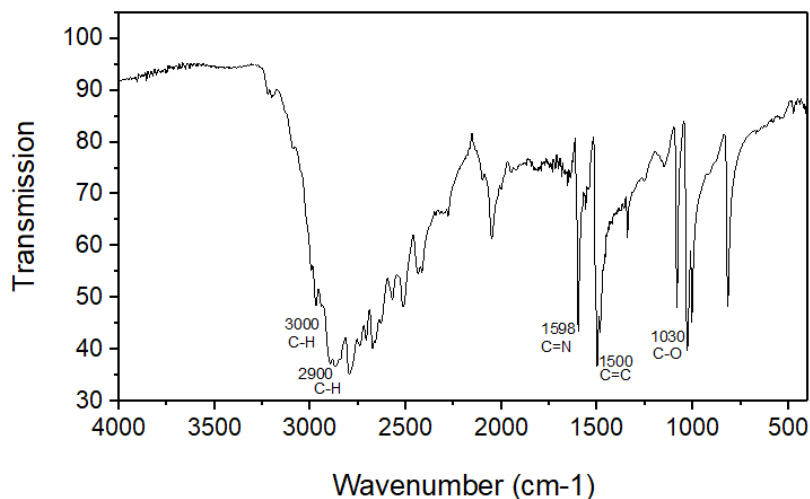


Figure 19. IR spectrum of complex 1.

The range in which the imine group is found (C=N) suggest that the ligand is bidentate,⁵⁷ this is different to the signal of aldehyde (C=O), the signal of the functional group Cl⁻ is not clear since some experimental evidence⁶¹ suggests the presence of this ligand with a higher signal. Thus, through IR analysis demonstrates the presence of ligand 1 coordinated to cobalt in complex 1.

3.3.4. UV-Vis Spectroscopy of complex 1.

In the complex 1, many peaks can be observed (Figure 20), there are peaks around 254 nm, 271 nm, 296 nm, also other peak with lowest absorbance around 490 nm.

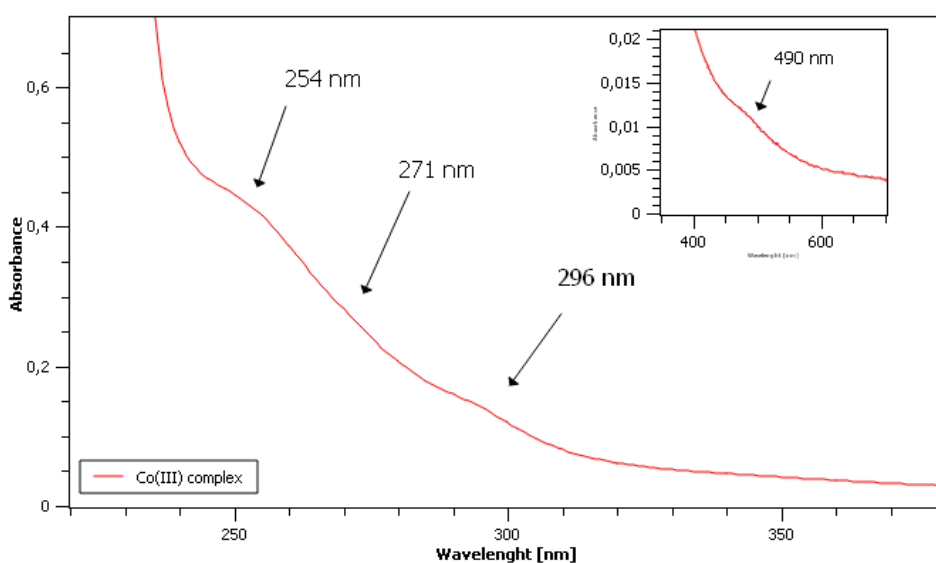


Figure 20. UV-Vis spectrum of complex 1. Insert: Spectrum of complex 1 in range 350-700nm.

The number of peaks is characteristic of d^6 metal configuration in Low Spin state according to Tanabe-Sugano diagram. The band around 254 nm could belong to $\pi-\pi^*$ transition from the aromatic rings, it is worth to note that these signals could be suffered a shift. The band around 490 nm is clearly a d-d transition that could correspond to $^1A_{1g} \rightarrow ^1T_{1g}$ transition, however the other two signals 296 and 271 nm could correspond to $^1A_{1g} \rightarrow ^1T_{2g}$, however the $^1A_{1g} \rightarrow ^1E_g$, $^1A_{1g} \rightarrow ^1A_{1g}(I)$ could be masked by the charge transfer transitions that stronger in the spectrum. This behavior is on UV-Vis spectra is found in other complexes of Low Spin cobalt(III)⁶² with similar geometry, which show clearly the first transition but the next transitions are difficult to distinguish by the charge transfer bands.

3.3.5. Remarks of proposed structures

The oxidation of cobalt(II) to cobalt(III) was clearly observed in the experimental measurements, in addition, it fulfilled what was expected when the ligands of the initial salt of $\text{CoCl}_2 \cdot 6\text{H}_2\text{O}$ were replaced by ligands that reduce the redox potential of this molecule with respect to the oxygen in the reaction. The preference of geometries that have certain metals such as cobalt(III) towards octahedral geometries as mentioned in the literature²⁵ could be seen in this complex and the measurements of effective magnetic moment and the UV-Vis spectrum confirmed this analysis.

The infrared spectroscopy gives us significant signals that evidences the presence of ligand 1, between these, the range value of signal of C=N corresponds to bidentate ligand. Some ligands coordinated to metal were discarded in a previous section, however, is not clear if the final compound have the presence of the chloride ligands, however the Low Spin behavior of the complex evidenced by the magnetic susceptibility and UV-Vis spectroscopy suggest the absence of such chlorides in the coordination sphere.

3.3.6 DNA extraction

This procedure was carried out through the method mentioned in previous section 2.8, the DNA obtained from this method is clearly showed in top of the test tube (Figure 21), with a white color.

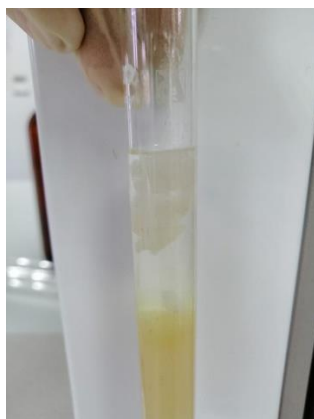


Figure 21. Vegetable DNA extracted.

The electronic absorption spectrum of the isolated DNA show bands around 260-280 nm (Figure 22), which is typical of DNA with a certain degree of free protein. $A_{260}:A_{280}$ ratio is equal to 1.6, this indicate sufficiently purity of DNA for the use in binding with complexes,⁴² however, slightly contamination is evidenced by the absence of a minimum at 234 nm characteristic of DNA, this can be associated to the presence of protein or polysaccharide contamination typically observed in DNA from plants.⁶³

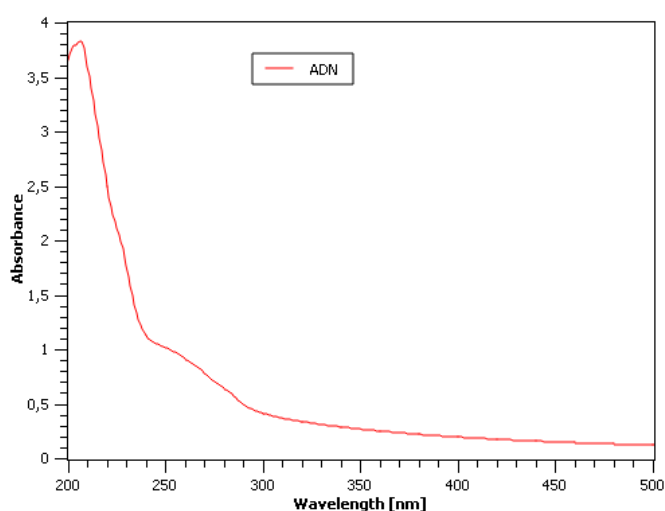


Figure 22. UV-Vis Spectrum of vegetable DNA

3.3.7 DNA binding with the complex 1.

In the UV-Vis spectrum of the mixture of complex 1 with DNA (Figure 23), the hypochromic effect expected⁵⁰ in the range of 260-280 nm does not appear in the spectrum, the increasing amounts of DNA, produce an increase of absorbance of the

mixture with the complex (hyperchromic effect). This could be by the excess of quantity added of DNA,⁴³ the lack of the π -stacking interactions or denaturation of DNA that show a typical hyperchromic effect, however, it is clear that binding is not favored under these conditions.

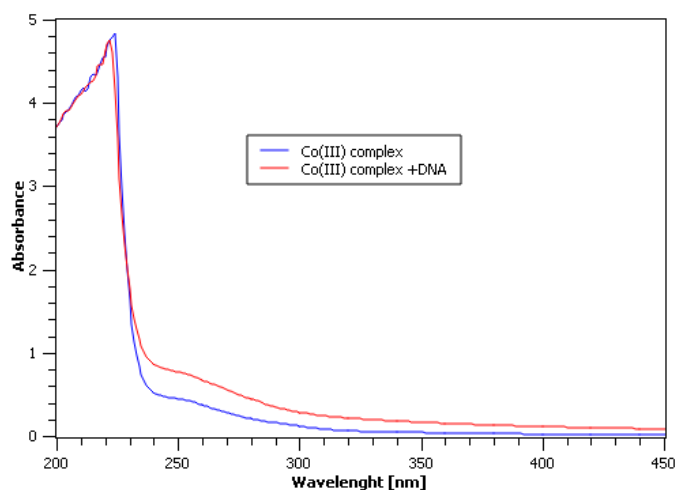


Figure 23. UV-Vis spectrum of cobalt(III) complex 1, blue line represents the only metal complex signal and red line shows the increases in amount of DNA.

3.4. Cobalt complex with ligand based on cinnamaldehyde (complex 2).

This synthesized cobalt complex was obtained after 12 hours under reflux conditions. The complex did not precipitate; hence, the use of bulky precipitant agent was necessary. The product was obtained with a sodium tetraphenylborate precipitant agent dissolved in the same solvent used in the reaction (methanol). By adding a few drops of this solution, the dark orange precipitated appeared immediately (Figure 24).



Figure 24. Synthesized complex of cobalt(III) with cinnamaldehyde.

The possibilities of coordination between the metal and ligands are showed in the Figure 25. The most probable geometry is tetrahedral, and it will be discussed in the next sections.

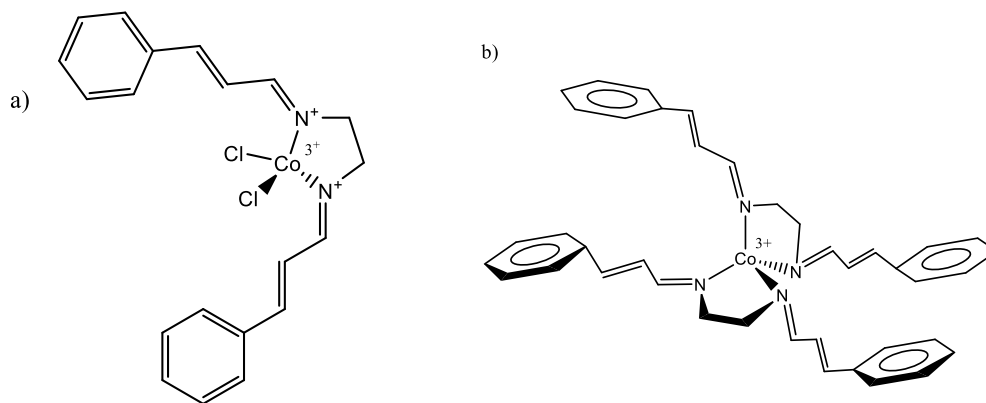


Figure 25. a) and b) are proposed structures of complex 2.

3.4.1. Characterization of complex 2 by magnetic susceptibility.

The experimental values to calculate the value of mass susceptibility of complex 2 were measured at room temperature, and the obtained values are showed in Table 2.

Table 2. Experimental values of complex 2 obtained from magnetic susceptibility balance.

	m_{empty} (g)	m_{full} (g)	R_o	R	L (cm)	C
Complex 2	0.8360	0.8852	-35	40	1.9	0.97

The value of C is calculated with the equation 3 previously mentioned. The experimental values of magnetic susceptibility per gram was obtained with the equation 4 is: $2.8095 \times 10^{-6} \text{g}^{-1}$.

With the purpose of calculate the experimental value of μ_{eff} is necessary the equation 6,

$$\mu_{eff} = 2.828\sqrt{\chi_{corr} \cdot T} \quad (6)$$

where χ_{corr} is the value of molar susceptibility (χ_M) minus diamagnetic corrections, and T is the temperature at which the experiment was performed. The calculated values of χ_M , χ_{corr} and μ_{eff} from the experimental measurements are showed in Table 3.

Table 3. Calculated values of χ_M , χ_{corr} , μ_{eff} from complex 2.

	Molecular Weight (g/mol)	χ_M (emu mol ⁻¹)	Diamagnetic corrections ⁶⁴ (emu mol ⁻¹)	χ_{corr} (emu mol ⁻¹)	μ_{eff} (BM)
Complex 2	1274.19	3.58×10^{-3}	-8.28×10^{-4}	4.41×10^{-3}	3.26

*emu=electromagnetic unit

The experimental values obtained of μ_{eff} and the theoretical values of μ_{eff} are compared to define some characteristics of metal complex. In this complex the experimental value obtained is $\mu_{eff} = 3.26$ BM.

3.4.2. Crystal Field Theory

With the supporting of Crystal Field Theory (Figure 26), the theoretical values of μ_{eff} can be calculated using the equation 5.

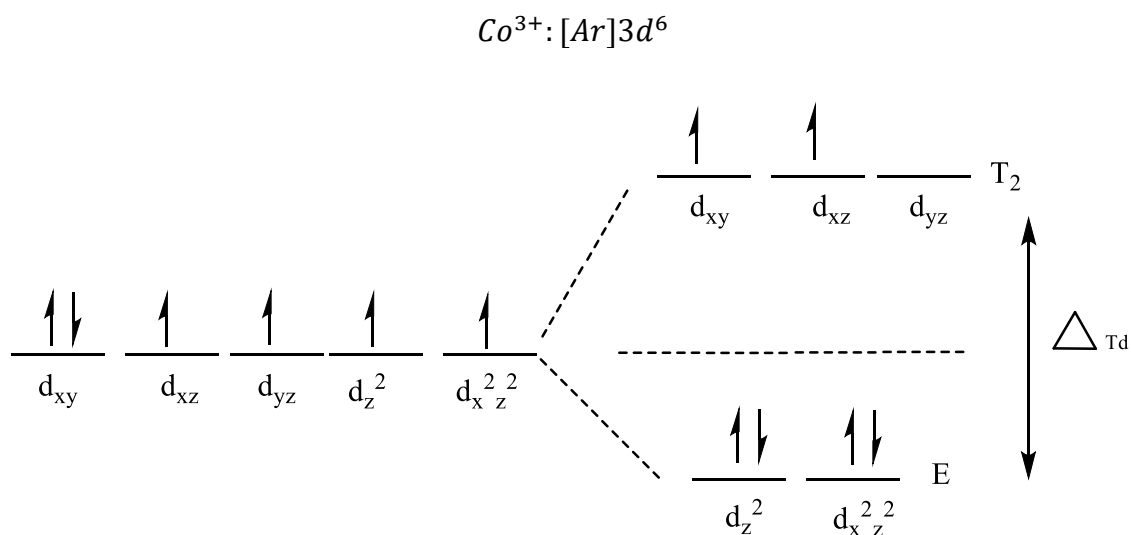


Figure 26. Tetrahedral Crystal Field of complex 2.

Using the spin orbital coupling to cobalt(II) and cobalt(III), the equation 5 is modified to equation 7:

$$\mu_{eff} = 2\sqrt{S(S + 1) + L(L + 1)} \quad (7)$$

where S is the number of unpaired electrons divided by two, and L is the nuclear magnetic moment and it is equal to 1. The μ_{eff} value obtained from equation 7 is showed in Table 4.

Table 4. Possible values to μ_{eff} from complex 2.

Metal	μ_{eff} theoretical values (BM)	
	CASE 1	CASE 2
Co ²⁺	3.87	
Co ³⁺		3.3166

From the analysis of the theoretical values (Table 4), the cobalt(II) with 3 unpaired electrons that has 3.87 BM value in d^7 species is close to our experimental value, however, using the equation of Spin-Orbit Coupling to cobalt(III) case (equation 7), the theoretical value of μ_{eff} increase from 1.78 BM (only spin) to 3.3166 BM (spin orbit) and it could be associated to 1 unpaired electron, and the last value is nearest to the experimental value.

In this complex, there are two possibilities very close to the experimental value. However, the case 2 is close to the experimental value that corresponds to cobalt (III). This fact is supported by the tendency of hexaaqua-cobalt(II) to oxidize, by oxygen from air, to cobalt (III) when aqua ligands are changed to nitrogen donor ligands (Schiff base) as was explained previously (Figure 18).

3.4.3. Infrared spectroscopy of complex 2

The IR spectrum of complex 2 (Figure 27) shows bands corresponding to ligand with some shift in signals. A band around 1590-1580 cm^{-1} mean the presence of imine ($\text{C}=\text{N}$),^{50,57-59} 3056-3050 cm^{-1} stretch for sp^2 $\text{C}-\text{H}$ band in aromatics,⁵⁹ around 1560 cm^{-1} to phenyl rings group($\text{C}=\text{C}$),⁵⁹ bands of the tetraphenyl borate are present but with light shifts,^{65,66} the absence of bands on 3600-3200 cm^{-1} shows that there are not $-\text{OH}$ and H_2O like ligands,⁵⁷ the absence bands of $\text{C}=\text{O}$ and $\text{C}-\text{O}$ show that there is not methoxy group of the initial aldehyde nor the presence of acetate group coordinated to metal, and the absence of $\text{N}-\text{H}_2$ band show that there are not ethylenediamine. Finally, 780-674 cm^{-1} band could correspond to signals of $-\text{Cl}$ ligand, however this value is highly sensitive to metal, quantity of this ligand and geometry, therefore the presence of this is not clear.^{60,61} The low intensity of the signals could be by the purity of the complex,⁶⁷ hence the relative concentration of the complex could be decreasing the intensity of peaks.

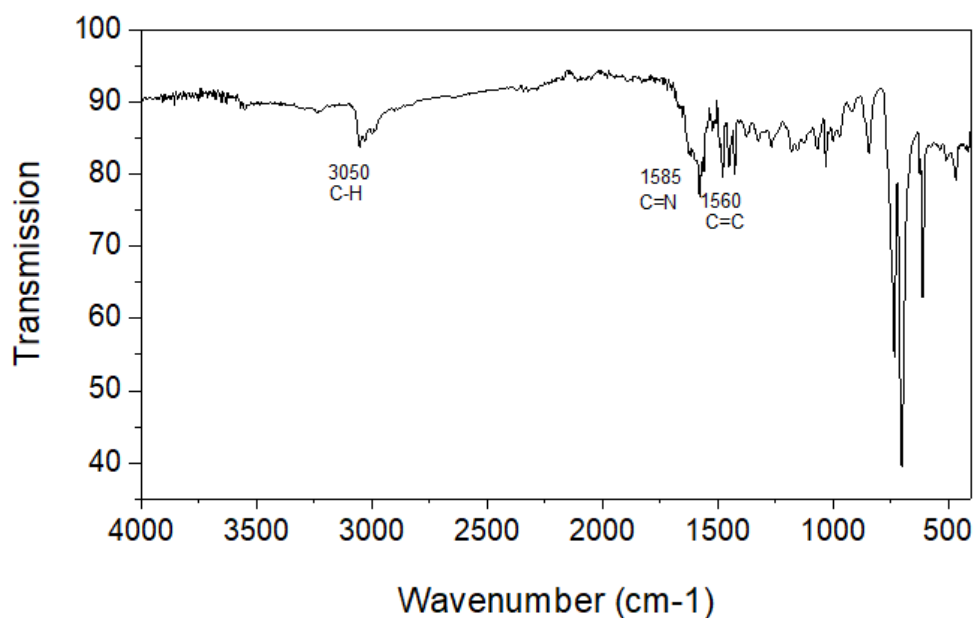


Figure 27. IR spectrum of complex 2.

The IR signals obtained in this complex belonging to the $\text{C}=\text{N}$ imine signal clearly differ from the $\text{C}=\text{O}$ signal shown in the initial aldehyde spectrum (Figure 8), this is the main evidence of the formation of imine group by the mechanism of reductive amination as

shown in the Figure 7, in addition, the range in which this signal occurs suggest a bidentate coordination.⁵⁷ Another important signal that the spectrum shows is the signal belonging to the C=C of the aromatic rings, this shows the presence of this as part of the ligand as mentioned in several articles.⁵⁹ Finally, the band that is shown between 780-674 cm^{-1} that could be attributed to Cl^- ,⁶⁰ in some books shows us that metals coordinated to metal Cl^- show bands 300-200 cm^{-1} ,⁵⁷ however in some experimental studies with cobalt⁶¹ they show it as the functional group of Cl^- directly coordinated to the metal.

Sodium tetraphenylborate

The use of Sodium tetraphenylborate as counter ion in the complex 2 is necessary to precipitate the complex, this suggest that the complex is cationic and the coordination of ligands differ of previous reports in literature.⁵¹

3.4.4. UV-Vis Spectroscopy of complex 2.

The electronic spectrum of complex 2 (Figure 28) show many peaks at different wavelengths, however the second group only can be shown in a very low absorbance window (Figure 28 insert). The first group show peaks at 266nm, 275nm, 293nm while the second group in low absorbance show peaks on 555 nm, 682 nm.

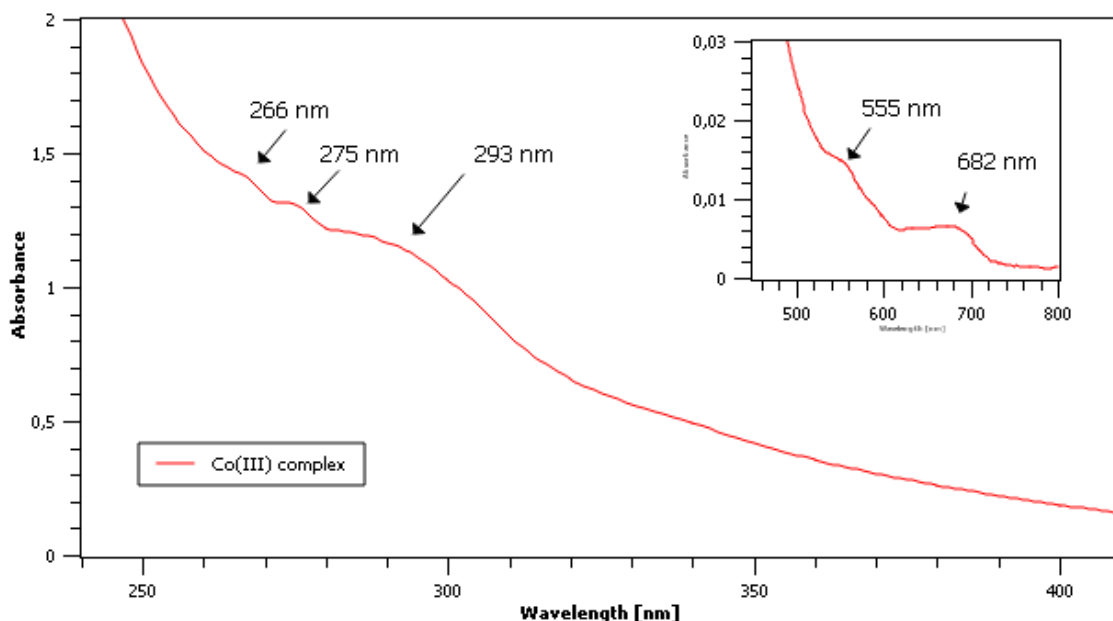


Figure 28. UV-Vis spectrum of complex 2. Insert: Spectrum of complex 2 in range 460-800 nm.

In order to assign the transitions through the Tanabe-Sugano Diagrams is necessary to apply the rule that change octahedral to tetrahedral diagrams (d^n tetrahedral = d^{10-n} octahedral), the quantity of peaks is similar to d^4 metal configuration in Low Spin according to Tanabe-Sugano Diagrams, it is a paramagnetic species, without take account the first peak whose intensity of absorbance and the range show that the electronic transition belongs to a charge transfer and so intense band, the band around 266 nm due to π - π^* transition belong to aromatic rings. The band around 682 nm is clearly a d-d transition that corresponds to ${}^3T_{1g} \rightarrow {}^3E_g$ transition, the signal around 555 nm corresponds to ${}^3T_{1g} \rightarrow {}^3T_{2g}$ (d-d transition), however the next signal around to 293 nm could correspond to next transition ${}^3T_{1g} \rightarrow {}^3A_{1g}$ but the next signal could be masked by high signals corresponds to charge transfer.

3.4.5. Remarks of proposed structures

In the case of complex 2, an oxidative behavior similar to complex 1 is expected, in which the metal passes from cobalt(II) to cobalt(III) due to its redox potential. The IR spectroscopy shows the signal of C=N very close to the range of bidentate imine ligand, for which the double coordination of the metal with the synthesized ligand is proposed.

The geometry suggested by the magnetic moment is tetrahedral, which is verified by UV-Vis spectroscopy. Although the information through the infrared spectrum is not clear about the coordination with chlorine, the peaks in UV-Vis spectroscopy suggest that it is a compound in Low Spin state, however, the presence of chlorine would lead to a High Spin behavior. In addition, by the fact that this complex was obtained through precipitation with a bulk anion (as precipitating agent), it gives us the idea that the chloride did not manage to stabilize the charge of the complex.

3.4.6. DNA binding with the complex 2.

In the UV-Vis spectrum of the mixture of complex 2 with DNA (Figure 29), the hypochromic effect expected⁵⁰ in the range of 260-280 nm is clear, the increasing amounts of DNA achieve to the decrease of the absorbance of the mixture with the complex. The increases of DNA show a percentage of hypochromism (%H) around 39.3%, also, a slightly bathochromic effect is showed in the bands of spectrum. To the calculations must be taken into account that although the values of binding constant (K_b) are obtained from equation 2, however, K_b is calculated comparing the equation of a line with equation 2, and K_b comes from the trend line shown by these values. Therefore, while more measurements are obtained, the approximation will be better, and from only two measurements the points form a line and a reliable value is not obtained. But, the %H show that there is an interaction with DNA biomolecules.

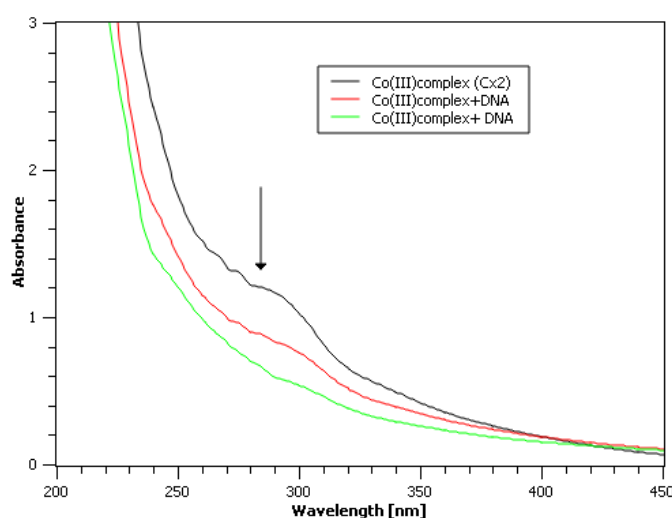


Figure 29. UV-Vis spectrum of cobalt(III) complex 2, black line represents only metal complex signal, and red and green lines show the successive increases in amounts of DNA.

3.5. Iron complex with ligand based on *p*-anisaldehyde (complex 3).

This synthesized iron complex 3 was obtained after 12 hours under reflux conditions, and this was vacuum filtered. The obtained product was shiny brown color (Figure 30).



Figure 30. Synthesized complex of iron(III) with *p*-anisaldehyde.

The possibilities of coordination between the metal and ligands are showed in the Figure 31. The most probable is octahedral geometry, and it will be discussed in the next sections.

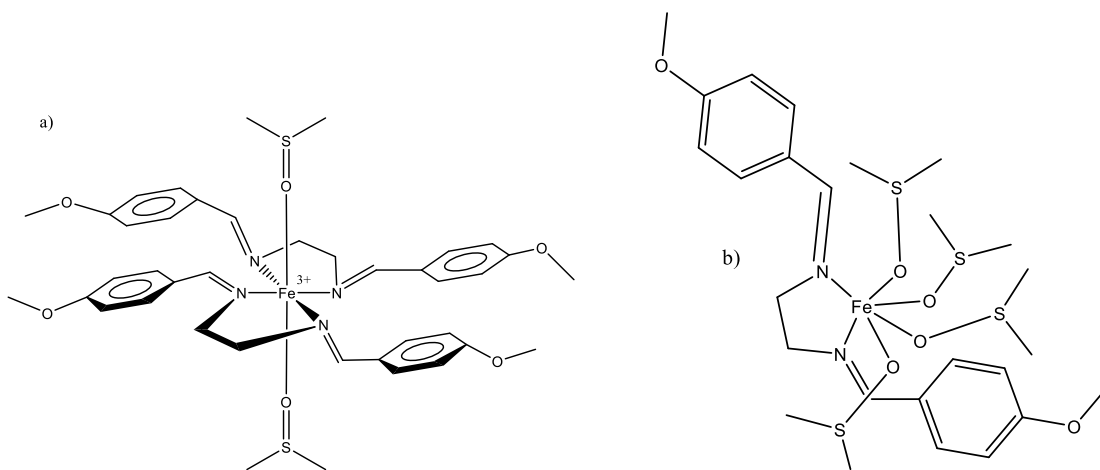


Figure 31. a) and b) are proposed structures of complex 3.

3.5.1. Characterization of complex 3 by magnetic susceptibility.

The experimental values to determine the value of mass susceptibility of complex 3 were measured at room temperature, and the obtained values are showed in Table 5.

Table 5. Experimental values of complex 3 obtained from magnetic susceptibility balance.

	m_{empty} (g)	m_{full} (g)	R_o	R	L (cm)	C
Complex 3	0.8338	0.9072	-35	168	1.9	0.97

The value of C is calculated with the equation 3 previously mentioned. The experimental values obtained to magnetic susceptibility per gram with the equation 4 is: $5.0971 \times 10^{-6} \text{g}^{-1}$, this value of complex 3 suggest a paramagnetic compound.

The values of χ_M , χ_{corr} , and μ_{eff} are showed in Table 6, and will be discussed in the next section.

Table 6. Calculated values of χ_M , χ_{corr} , μ_{eff} from complex 3.

	Molecular Weight (g/mol)	χ_M (emu mol ⁻¹)	Diamagnetic corrections ⁶⁴ (emu mol ⁻¹)	χ_{corr} (emu mol ⁻¹)	μ_{eff} (BM)
Complex 3	990.8597	5.05×10^{-3}	-5.45×10^{-4}	5.6010^{-3}	2.58

The experimental values obtained of μ_{eff} and the theoretical values of μ_{eff} are compared to define the electronic state of the metal complex. In this complex the experimental value obtained is $\mu_{eff} = 2.58$ BM. This experimental value is compared with the theoretical values obtained from Crystal Field Theory.

3.5.2. Crystal Field Theory

With the supporting of Crystal Field Theory (Figure 32), the theoretical values of μ_{eff} can be calculated using the equation 5. The theoretical values of $\mu_{eff} = 5.91$ BM to High Spin of iron(III), when comparing these values there is a difference in magnetic moment, however this change could be related to a possible antiferromagnetic behavior shown by the synthesized complex, causing the value of magnetic moment to drop due to the disposition that they can adopt with the magnetic field.

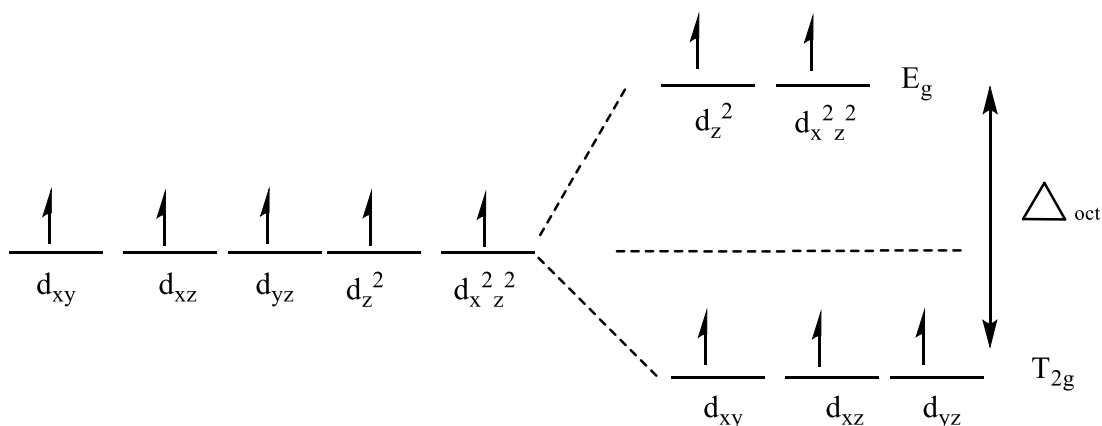
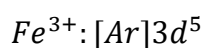


Figure 32. Octahedral Crystal Field of complex 3.

Comparing with the theoretical value it can be associated to Fe(III) with the case having 5 unpaired electrons it has a magnetic moment of 5.8 BM expected for a d^5 species, however, the value is lower than theoretical value as it usually occurs in this type of complex .

3.5.3. Infrared spectroscopy of complex 3

The IR spectrum of complex 3 (Figure 33) show a weak band on 1516 cm^{-1} could be the imine signal with shift, the 1380 cm^{-1} and 1291 cm^{-1} could correspond to phenyl group, 2970 cm^{-1} signal C-H sp^3 , 3115 cm^{-1} band corresponds to =C-H sp^2 , and around 1015 cm^{-1} band corresponds to DMSO (S-O)⁶⁸ with a light shift of the typical value. The band around 820 cm^{-1} associated to *-para* substitution.

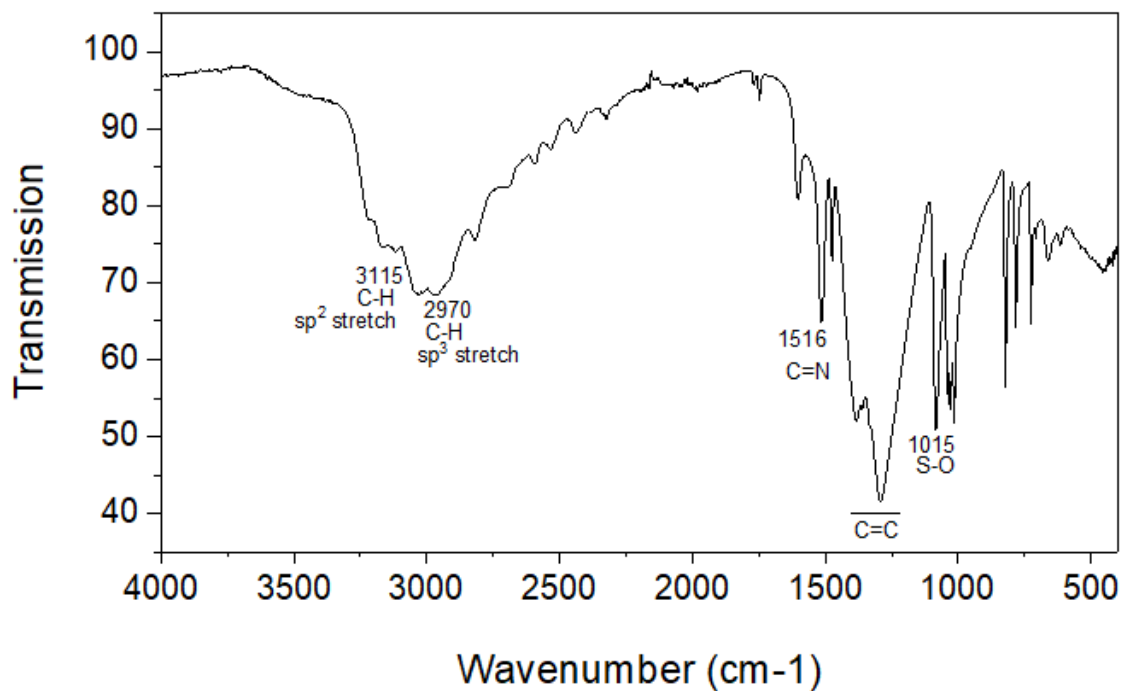


Figure 33. IR spectrum of complex 3.

The S-O signals shown indicate a clear presence of the DMSO substituent in the complex, in addition, although the signal that should correspond to the imines shows shift, the presence of the aldehyde is ruled out by the absence of the characteristic C=O signal around 1700 cm⁻¹.

3.5.4. UV-Vis Spectroscopy of complex 3.

In the spectrum of complex 3 (Figure 34) two peaks are observed at 228 nm and 275 nm. The red line shows the only absorbance of the complex.

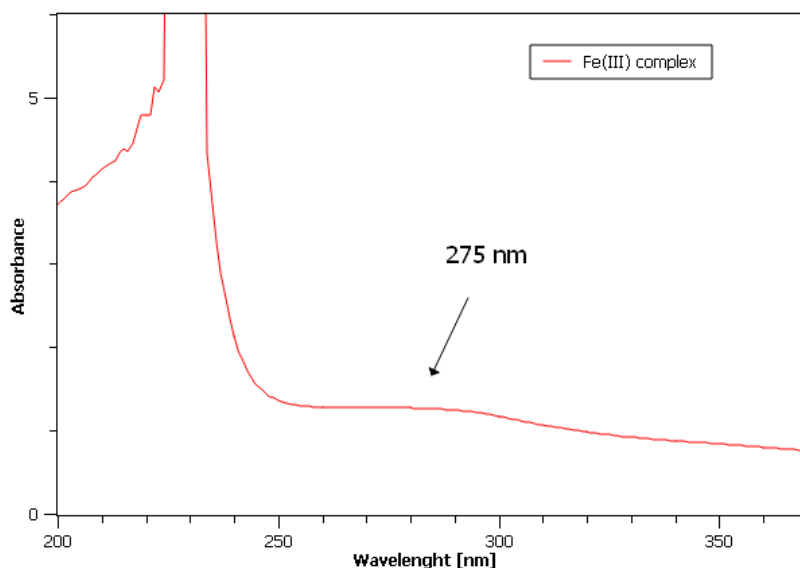


Figure 34. UV-Vis spectrum of complex 3.

The peak around 228 nm is assigned to a charge transfer due to the range in which it is presented and its high absorbance, the peak around 275 nm is referred to π - π transition of aromatic compounds. The absence of other peaks in Visible region is characteristic of a d^5 High Spin species.

3.5.5. Remarks of proposed structures

This complex is evidenced as an octahedral complex of iron(III) High Spin (d^5 HS), where the experimental value of magnetic susceptibility differs from the theoretical value due probably to an antiferromagnetic influence. This is supported by the UV-Vis spectrum that shows an absence of d-d transitions as would be expected for a High Spin d^5 species, however it shows a band that could be attributed to the ligand. Although it is not clear how many ligands are present in the complex, the chelate effect could influence a greater stability of the molecule by the coordination of two bidentate ligand.

3.5.6. DNA binding with the complex

In the UV-Vis spectrum of the mixture of complex 3 with DNA (Figure 35), the hypochromic effect expected⁵⁰ in the range of 260-280 nm is clear in the spectrum, the increasing amounts of DNA achieve to the decrease of the absorbance of the mixture with the complex. The first increase of DNA shows a percentage of hypochromism (%H) around 32.28%, also, a bathochromic effect is showed in bands of spectrum. To the

calculations must be taken into account that although the values of binding constant (K_b) are obtained from equation 2, however, K_b is calculated comparing the equation of a line with equation 2, and K_b comes from the trend line shown by these values. Therefore, while more measurements are obtained, the approximation will be better, and from only two measurements the points form a line and a reliable value is not obtained. But, the %H show that there is an interaction with DNA biomolecules.

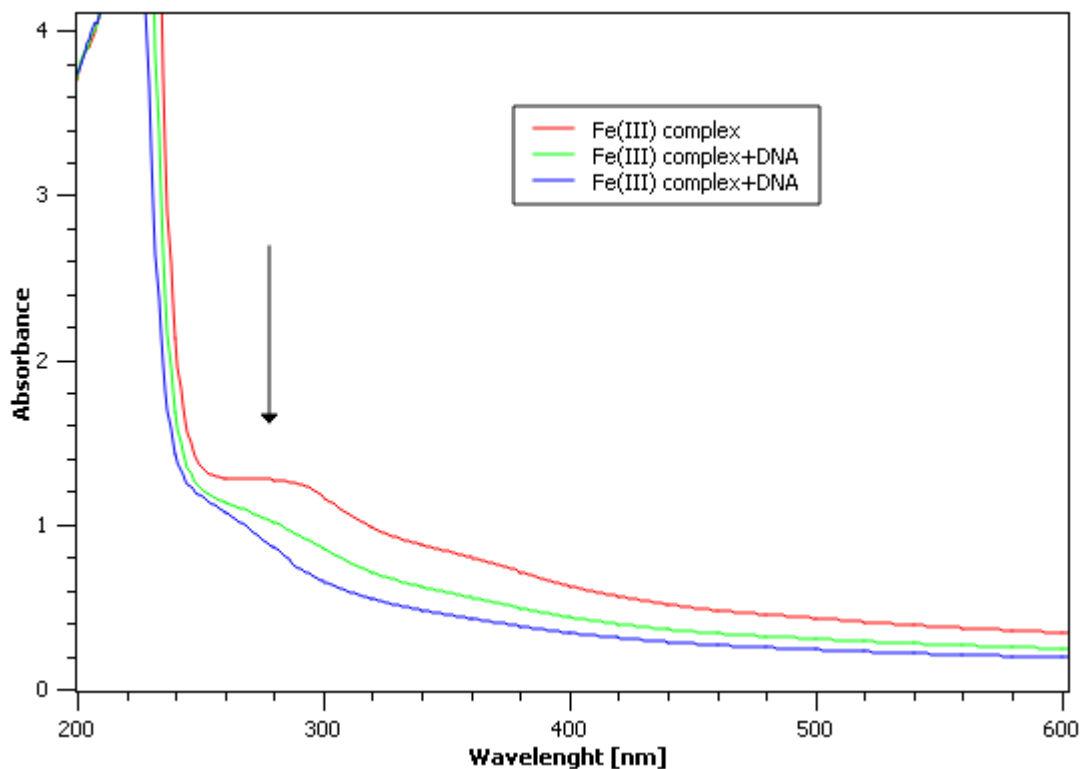


Figure 35. UV-Vis spectrum of iron(III) complex 3, red line represents only metal complex signal, and green and blue lines show the successive increases in amounts of DNA.

3.6. Iron complex with ligand based on cinnamaldehyde (complex 4).

This synthesized iron complex 4 was obtained after 12 hours under reflux conditions, and this was vacuum filtered. The obtained product was reddish brown color (Figure 36).



Figure 36. Synthesized complex of iron(III) with cinnamaldehyde.

The possibilities of coordination between the metal and ligands are showed in the Figure 37. The most probable is octahedral geometry, and it will be discussed in the next sections.

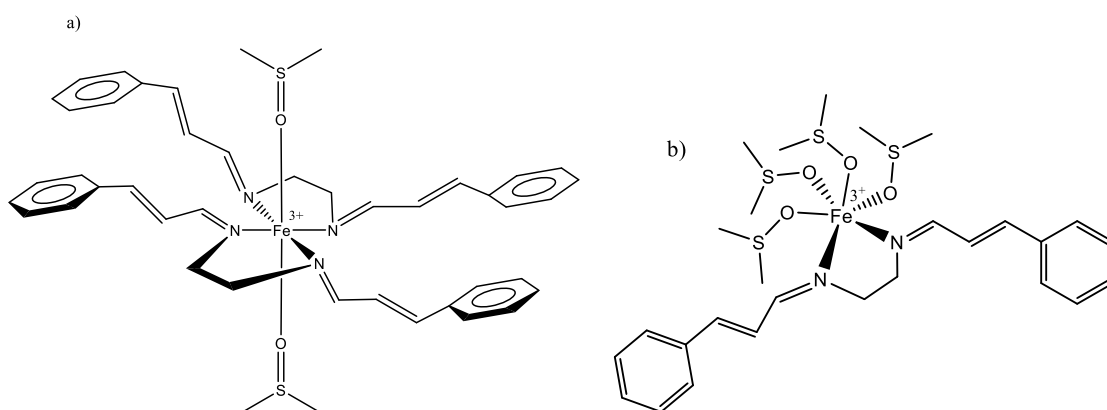


Figure 37. a) and b) are proposed structures of complex 4.

3.6.1. Characterization of complex 4 by magnetic susceptibility.

The experimental values to calculate the value of mass susceptibility of complex 4 were measured at room temperature, and the obtained values are showed in Table 7.

Table 7. Experimental values of complex 4 obtained from magnetic susceptibility balance.

	m_{empty} (g)	m_{full} (g)	R_o	R	L (cm)	C
Complex 4	0.1401	0.2486	-35	70	1.9	0.97

The experimental value obtained to magnetic susceptibility per gram with the equation 4 is: $1.7835 \times 10^{-6} \text{g}^{-1}$, this value of complex 4 suggest a paramagnetic compound.

The calculated values of χ_M , χ_{corr} and μ_{eff} are showed in Table 8, and they will be compared with the theoretical values in the next section.

Table 8. Calculated values of χ_M , χ_{corr} , μ_{eff} from complex 4.

	Molecular Weight (g/mol)	χ_M (emu mol ⁻¹)	Diamagnetic corrections ⁶⁴ (emu mol ⁻¹)	χ_{corr} (emu mol ⁻¹)	μ_{eff} (BM)
Complex 4	974.8997	1.74×10^{-3}	-5.5×10^{-4}	2.29×10^{-3}	1.65

3.6.2. Crystal Field Theory

With the supporting of Crystal Field Theory (Figure 38), the theoretical values of μ_{eff} can be calculated using the equation 5.

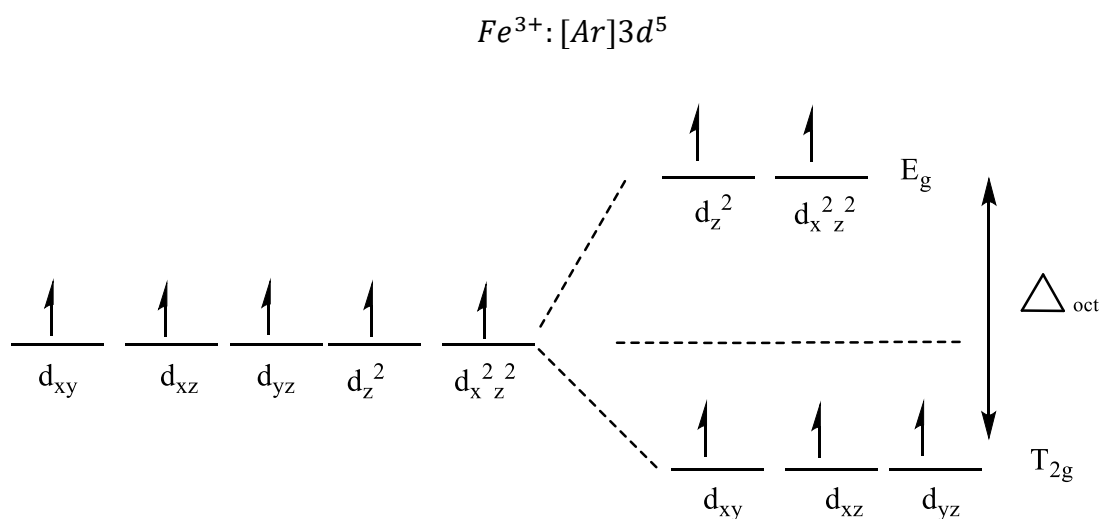


Figure 38. Octahedral Crystal Field of complex 4.

The μ_{eff} theoretical value obtained are showed in Table 9, and it is compared to define the geometry.

Table 9. Theoretical value of complex 4.

	$\mu_{eff} (BM)$
Metal	CASE 1
Fe ³⁺	5.91

The theoretical values of μ_{eff} to iron(III) are compared with experimental value of μ_{eff} , and it is nearest to case with only one unpaired electron. However, UV-Vis spectra show the absence of characteristics peaks to Low Spin species, and the peaks of this spectrum are the expected for d⁵ High Spin metal species. Therefore, the difference between the values could be due to an antiferromagnetic behavior of the complex that can decrease this magnetic moment.

3.6.3. Infrared spectroscopy of complex 4

The IR spectrum of complex 4 (Figure 39) show a broad band around 1580-1530 cm⁻¹, this band can be explained by the overlapping that corresponds to imine signal (C=N) and phenyl signal combined with other band around 1433-1401 cm⁻¹ (C=C), a characteristic band around 1030 cm⁻¹ identify the DMSO (S-O) stretch.⁶⁸

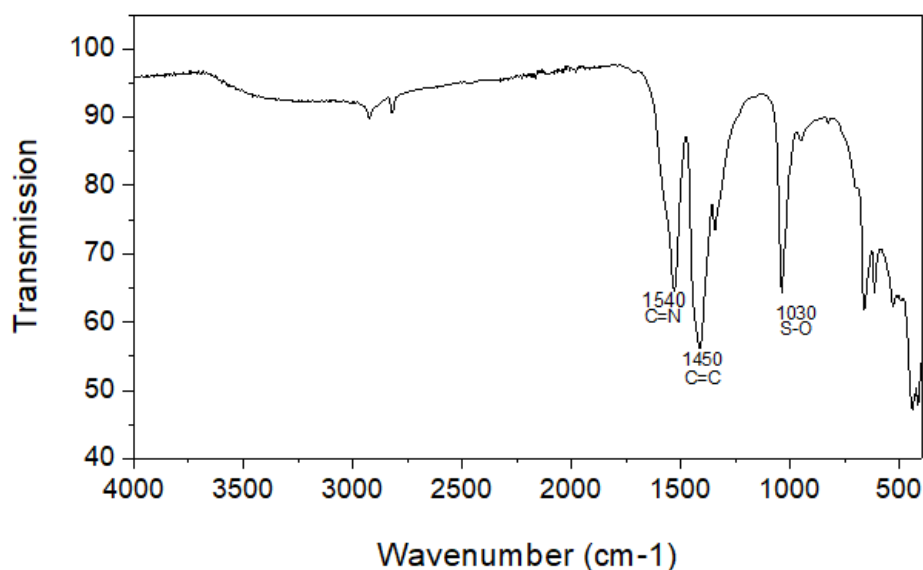


Figure 39. IR spectrum of complex 4.

In this compound, the C=N signal shows a slight shift in the imine group, the signals of the phenyl groups are strong and wide, remembering that here the C=C signal belonging to the double bond outside the ring could be modified or overlapped aromatic.

3.6.4. UV-Vis Spectroscopy of complex 4.

In the spectrum of complex 4 (Figure 40), two peaks are showed, peak around 214 nm with high absorbance and so broad peak between 250-330 nm. The red line shows the absorbance of complex.

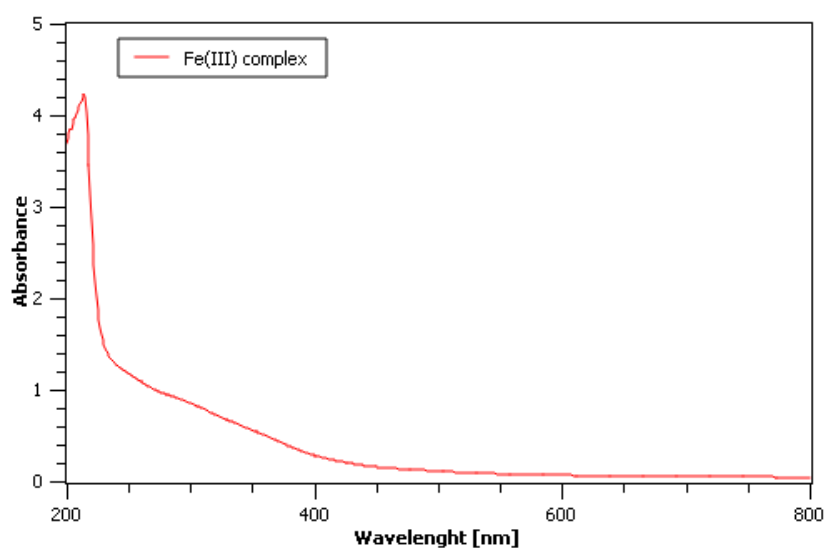


Figure 40. UV-Vis spectrum of complex 4.

The electronic transitions on d^5 High Spin species are not allowed, this fact is evidenced in Tanabe Sugano Diagram where ${}^6A_{1g}$ does not has excited state with the same multiplicity. This fact is clear in this complex since in the experimental spectrum, the peak around 214 nm belongs to charge transfer, the broad band between 250-330 nm is difficult to distinguish the electronic transition, however, due to the nature of ligand is possible the presence of band belongs to $\pi-\pi^*$ of aromatic rings.

3.6.5. Remarks of proposed structures

The synthesized complex 4 shows an octahedral geometry, also show that metal is iron(III) of High Spin (d^5 HS), where although the experimental value of magnetic susceptibility differs from the theoretical value expected for this compound, and although it could thinking it has antiferromagnetic influence, the value is still small

compared to the theoretical. However, the measurement through the UV-Vis spectrophotometer shows an absence of transitions as would be expected for a High Spin d^5 species thus confirming the High Spin state of iron(III). Furthermore, this spectrum shows a very broad band in the UV region that could be attributed to the ligand since it is at the point of interaction with DNA. Although in this case it is also difficult to determine the entire structure of the complex, the chelate effect could influence a greater stability of the molecule in which it has more imine binders attached to it, in addition to being more symmetrical.

3.6.6. DNA binding with the complex

In the UV-Vis spectrum of the mixture of complex 4 with DNA (Figure 41), the hypochromic effect expected in the range of 260-280 nm is not clear because the first increase of DNA (green) almost keeps the position, but with the next increase of DNA the absorbance increases too. In this case, calculate the values of binding constant (K_b), and the hypochromic effect (%H) are not possible because the addition of DNA seems that produce an hyperchromic effect.

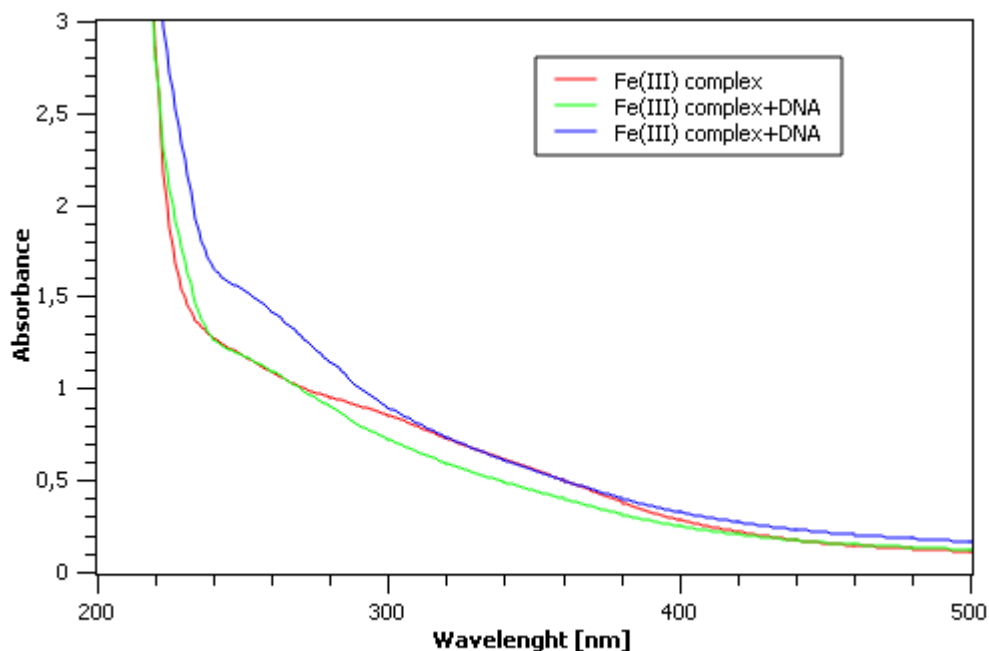


Figure 41. UV-Vis spectrum of iron(III) complex 4, red line represents only metal complex signal, and green and blue lines show the successive increases in amounts of DNA.

The observed effect with the increases of DNA looks like a hyperchromic effect that could be caused by the excess of quantity added of DNA,⁴³ the lack of the π -stacking interactions or denaturation of DNA that show a typical hyperchromic effect. Here, it appears that the excess of the increased amount of DNA produced the increase in absorbance. The spectrum show that binding is not favored under these conditions, but it can be tested with lower increases of DNA to the complex.

3.7. Docking studies of synthesized ligands using Autodock software

3.7.1. Interaction with ligand based on *p*-anisaldehyde

The docking simulations were carried out on this ligand allow to analyze the affinity that it could have with DNA biomolecules, which would lead to potential uses as anticancer agents associated with reaction mechanisms based on intermolecular interactions as π - π stacking.

This docking results shows 10 possible conformations and the positions in which it could interact with the ligand. The conformation with lower binding energy is showed Figure 42.

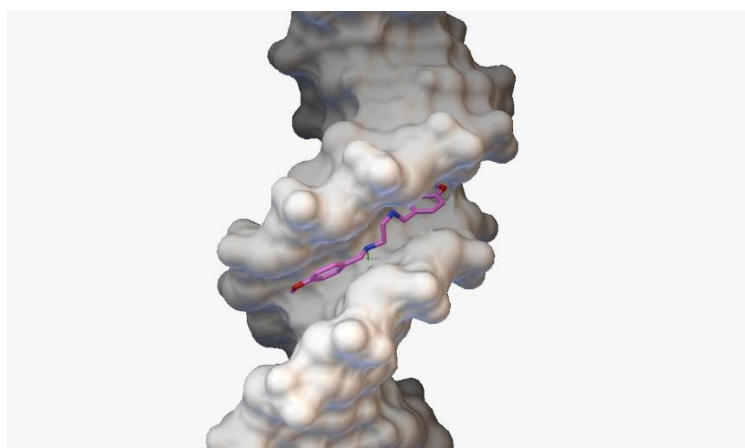


Figure 42. Interaction of ligand based on *p*-anisaldehyde with 1BNA DNA.

In the conformation with lower binding energy at room temperature, the results obtained are showed in Table 10.

Table 10. Results of docking with autodock of ligand 1.

	Estimated Free Energy (kcal/mol)	Final Intermolecular Energy (kcal/mol)	Van der Waals + Hydrogen bond + Desolvation Energy (kcal/mol)	Inhibition Constant (nM)
Ligand 1	-8.61	-10.70	-10.60	489.36

Figure 43 shows the hydrogen bond between ligand based on *p*-anisaldehyde with 1BNA sequence, also, an important fact shown by the docking is that in the analysis of intercalation with ligand, the interaction seems to be mediated by intermolecular forces (probably π - π interaction) instead of covalent bonding.

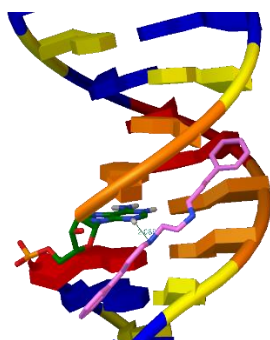


Figure 43. Hydrogen bond from docking with ligand 1.

3.7.2. Interaction with ligand based on cinnamaldehyde

This docking shows 10 possible conformations and the positions in which it could interact with the ligand. The conformation with lower binding energy is shown in Figure 44.

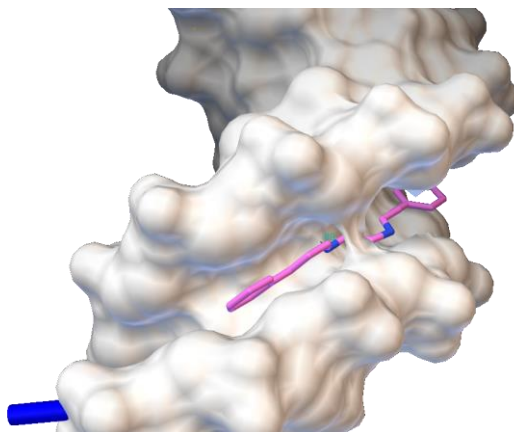


Figure 44. Interaction of ligand based on cinnamaldehyde with 1BNA sequence.

In the conformation with lower binding energy at room temperature, the results obtained are showed in Table 11.

Table 11. Results of docking with autodock of ligand 2.

	Estimated Free Energy (kcal/mol)	Final Intermolecular Energy (kcal/mol)	Van der Waals + Hydrogen bond + Desolvation Energy (kcal/mol)	Inhibition Constant (nM)
Ligand 2	-9.95	-12.04	-12.03	50.65

Figure 45 shows the hydrogen bond between ligand based on cinnamaldehyde with 1BNA sequence, also, an important fact shown by the docking is that in the analysis of intercalation with ligand, the interaction seems to mediated by intermolecular forces (probably π - π interaction) instead of covalent bonding.

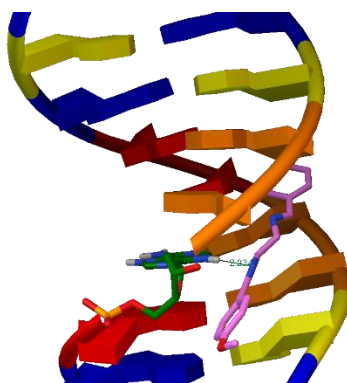


Figure 45. Hydrogen bond from docking with ligand 2.

3.8. Docking studies of synthesized complexes using Hex 8.0.0 software.

3.8.1. Cobalt complex with ligand based on *p*-anisaldehyde (complex 1).

This docking was carried out between complex 1 (figure 16a) with 1BNA. The figure 46a shows the most stable position among the probable orientations due to its total energy of -374 kJ/mol, this without the possibility of a cisplatin-type interaction with 1BNA because the complex has not labile ligands, and H-bonds are not shown. This fact could mean the probable presence of π stacking interactions between the complex and the biomolecule, also figure 46b shows the atoms belong to the chains that are closest to the complex.

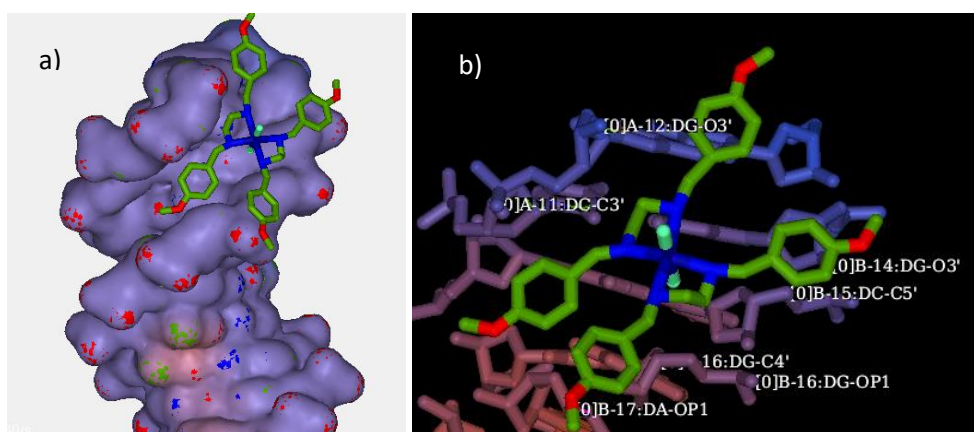


Figure 46. Docking of complex 1 with 1BNA. a) Solid Surface of 1BNA with complex, b) Closest atoms of the 1BNA chain with the complex.

3.8.2. Cobalt complex with ligand based on cinnamaldehyde (complex 2).

This docking was carried out between complex 2 (figure 25b) with 1BNA. The figure 47a shows the most stable position among the probable orientations due to its total energy of -350 kJ/mol, the same fact that in last complex support the possible presence of π stacking interactions, also figure 47b shows the atoms belong to the chains closest to the complex. One important fact is that the total energy is different between the two cobalt complexes.

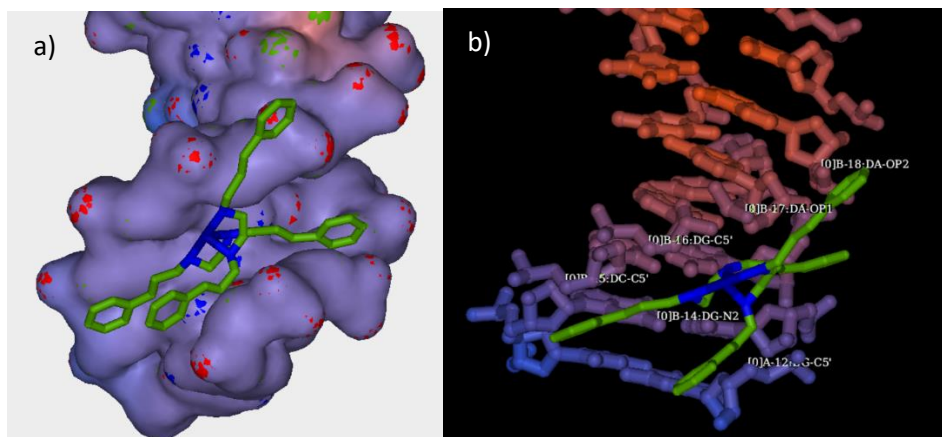


Figure 47. Docking of complex 2 with 1BNA. a) Solid Surface of 1BNA with complex, b) Closest atoms of the 1BNA chain with the complex.

3.8.3. Iron complex with ligand based on *p*-anisaldehyde (complex 3).

This docking was carried out between complex 3 (figure 31a) with 1BNA. The figure 48a shows the most stable position among the probable orientations due to its total energy of -386 kJ/mol, the same fact that in last complexes support the possible presence of π stacking interactions, also figure 48b shows the atoms belong to the chains closest to the complex. One important fact is that the total energy is higher than complex 3 that has the same ligand synthesized, it means more stability for the iron complex. Also, it has higher total energy than complex 2 that can be associated to geometry and the Schiff base ligand of the complex 2.

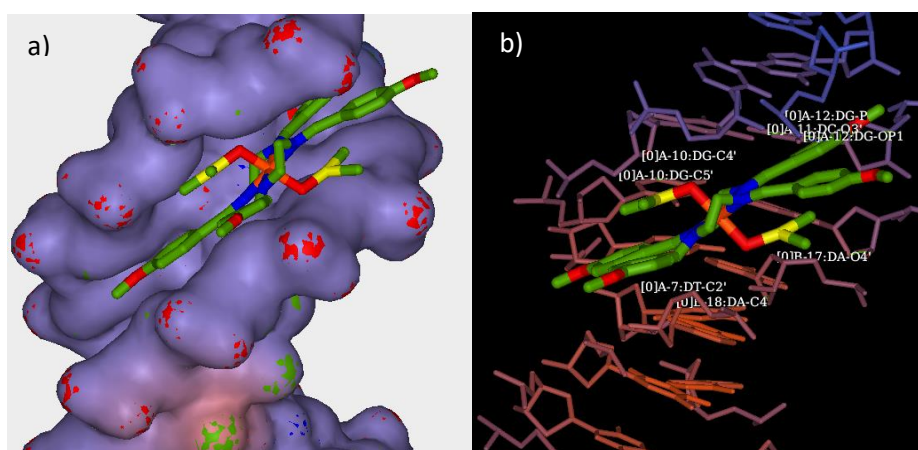


Figure 48. Docking of complex 3 with 1BNA. a) Solid Surface of 1BNA with complex, b) Closest atoms of the 1BNA chain with the complex.

3.8.4. Iron complex with ligand based on cinnamaldehyde (complex 4).

This docking was carried out between complex 4 (figure 37a) with 1BNA. The figure 49a shows the most stable position among the probable orientations due to its total energy of -350 kJ/mol, the same fact that in last complexes support the possible presence of π stacking interactions, also figure 49b shows the atoms belong to the chains closest to the complex. One important fact is that the total energy is the same that complex 2, it shows the directly dependance of the ligand without take account the difference in geometry, and the energy is different between two iron complexes.

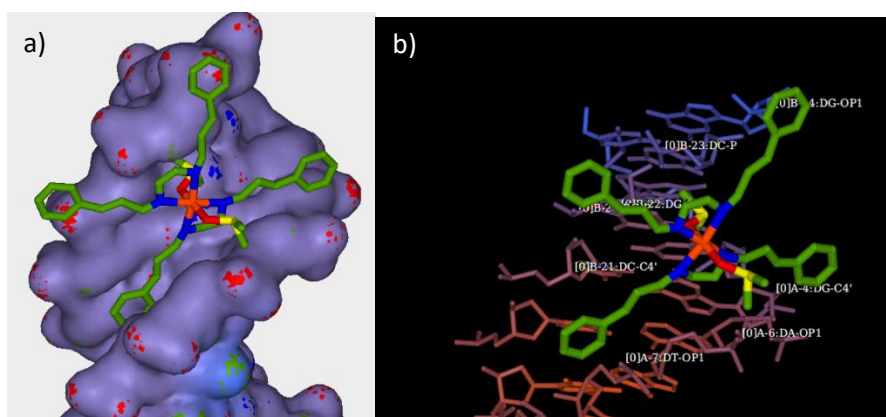


Figure 49. Docking of complex 4 with 1BNA. a) Solid Surface of 1BNA with complex, b) Closest atoms of the 1BNA chain with the complex.

Conclusions

The synthesis of metal complexes based on Schiff bases shows encouraging results when they interact with DNA. These complexes were characterized by techniques such as Infrared Spectroscopy, UV-Vis spectroscopy, and magnetic susceptibility.

Infrared Spectroscopy supports the presence of several functional groups in the complex such as signals of imines or aromatic rings and rules out the presence of signals from ethylenediamine or aldehydes. UV-Vis spectroscopy and magnetic susceptibility support the presence of the metal and its oxidation states in the metal complex.

Extraction of aldehydes from plants was successful and it allows to perform cheap synthesis of Schiff base ligands as in the case of cinnamaldehyde that was obtained from cinnamon bark. Structure of cinnamaldehyde was demonstrated through Infrared Spectroscopy analysis. The signals obtained from cinnamaldehyde agreed with the expected signals reported in literature, although the yield was not very high and the TLC plate showed the possible presence of impurities. In the next step of the design of the ligands, cinnamaldehyde and *p*-anisaldehyde were successfully condensed with ethylenediamine and formed the characteristic double bond of the imines (Schiff bases).

In the last step of the synthesis, four complexes derivate from the reactions of cobalt(II) with ligands 1 and 2 and from the reactions of iron(III) with ligands 1 and 2 were obtained. Spectroscopic analysis demonstrates the successfully coordination of the ligands giving place to the next complexes:

Complex 1: Option 1: Cobalt(III) Low Spin, two Ligands 1, two Cl⁻, Octahedral

Option 2: Cobalt(III) Low Spin, three Ligands 1, Octahedral

Complex 2: Cobalt(III) Low spin, two Ligands 2, Pseudotetrahedral

Complex 3: Iron(III) High Spin, two ligands 1, two DMSO, Octahedral

Complex 4: Iron(III) High Spin, two ligands 2, two DMSO, Octahedral

Vegetal DNA was extracted with success and used to interact with the synthesized complexes. The purity of DNA was analyzed with UV-Vis spectroscopy, where the ratio $A_{260}:A_{280}$ was equal to 1.6 which means that the DNA was not totally pure but it sufficiently to perform analysis.

The complexes were tested to interact with the extracted DNA, where **complex 2** and **complex 3** showed a clear interaction with DNA (hypochromic effect). **Complex 1** and **complex 4** showed no affinity to interact with DNA under the conditions of the experiment. The positive interactions shown by the **complex 2** and **3** with DNA could be associated with pi stacking interaction.

The docking studies shows that free ligands have a degree of affinity to bind with DNA, in both cases this effect is produced by intermolecular forces. The studies with the metal complexes 1 to 4 show a degree of affinity to DNA, but the complexes cannot bind directly like cisplatin and the docking were not showed H-bond. So that, the interactions could be produced by π stacking interactions. The experimental interactions and those obtained by simulation are encouraging since they show us a certain affinity to which complexes and ligands of this type could interact, which means high potentialities for uses in medicinal chemistry such as anti-cancer drugs, through mechanism similar to cisplatin and by the π stacking interactions.

Recommendations

- Perform more spectroscopic characterization in order to determine unambiguously the structure of the ligands and the complexes.
- Improve the method of obtaining DNA to increase its purity or carry out tests with commercially DNA.
- Further studies with cancer cell lines will be useful in order to evaluate the real anticancer properties of our complexes.
- Increase the number of tests performed with the UV-Vis spectrophotometer in which a greater number of successive increases of DNA are made to interact with the synthesized complex, and thus be able to obtain the binding constant with precision and also the percentage of hypochromism.

Perspectives

The previous results of binding with DNA are encouraging with two of the complexes, however tests under better conditions of interaction or directly with cancer lines could give us a more certain result about their potential as anticancer drugs.

References

- (1) Sudhakar, A. History of Cancer, Ancient and Modern Treatment Methods. *J. Cancer Sci. Ther.* **2009**, *01* (02), 1–4. <https://doi.org/10.4172/1948-5956.100000e2>.
- (2) Bray, F.; Ferlay, J.; Soerjomataram, I.; Siegel, R. L.; Torre, L. A.; Jemal, A. Global Cancer Statistics 2018: GLOBOCAN Estimates of Incidence and Mortality Worldwide for 36 Cancers in 185 Countries. *CA. Cancer J. Clin.* **2018**, *68* (6), 394–424. <https://doi.org/10.3322/caac.21492>.
- (3) Chen, W.; Zheng, R.; Baade, P. D.; Zhang, S.; Zeng, H.; Bray, F.; Jemal, A.; Yu, X. Q.; He, J. Cancer Statistics in China, 2015. *CA. Cancer J. Clin.* **2016**, *66* (2), 115–132. <https://doi.org/10.3322/caac.21338>.
- (4) Siegel, R. L.; Miller, K. D.; Jemal, A. Cancer Statistics, 2019. *CA. Cancer J. Clin.* **2019**, *69* (1), 7–34. <https://doi.org/10.3322/caac.21551>.
- (5) Miller, K. D.; Fidler-Benaoudia, M.; Keegan, T. H.; Hipp, H. S.; Jemal, A.; Siegel, R. L. Cancer Statistics for Adolescents and Young Adults, 2020. *CA. Cancer J. Clin.* **2020**, *70* (6), 443–459. <https://doi.org/10.3322/caac.21637>.
- (6) Miller, K. D.; Siegel, R. L.; Lin, C. C.; Mariotto, A. B.; Kramer, J. L.; Rowland, J. H.; Stein, K. D.; Alteri, R.; Jemal, A. Cancer Treatment and Survivorship Statistics, 2016. *CA. Cancer J. Clin.* **2016**, *66* (4), 271–289. <https://doi.org/10.3322/caac.21349>.
- (7) DeVita, V. T.; Chu, E. A History of Cancer Chemotherapy. *Cancer Res.* **2008**, *68* (21), 8643–8653. <https://doi.org/10.1158/0008-5472.CAN-07-6611>.
- (8) Chakraborty, S.; Rahman, T. The Difficulties in Cancer Treatment. *Ecancermedicalscience* **2012**, *6*, 1–5. <https://doi.org/10.3332/ecancer.2012.ed16>.
- (9) Richardson, J. L.; Marks, G.; Levine, A. The Influence of Symptoms of Disease and Side Effects of Treatment on Compliance with Cancer Therapy. *J. Clin. Oncol.*

1988, 6 (11), 1746–1752. <https://doi.org/10.1200/JCO.1988.6.11.1746>.

- (10) Sun, C. C.; Bodurka, D. C.; Weaver, C. B.; Rasu, R.; Wolf, J. K.; Bevers, M. W.; Smith, J. A.; Wharton, J. T.; Rubenstein, E. B. Rankings and Symptom Assessments of Side Effects from Chemotherapy: Insights from Experienced Patients with Ovarian Cancer. *Support. Care Cancer* **2005**, 13 (4), 219–227. <https://doi.org/10.1007/s00520-004-0710-6>.
- (11) Ahmad, S. S.; Reinius, M. A. V; Hatcher, H. M.; Ajithkumar, T. V. Anticancer Chemotherapy in Teenagers and Young Adults: Managing Long Term Side Effects. *BMJ* **2016**, 354, 1–8. <https://doi.org/10.1136/bmj.i4567>.
- (12) Steinmann, D. Late Effects After Radiotherapy. In *Late Effects After Radiotherapy BT - Late Treatment Effects and Cancer Survivor Care in the Young: From Childhood to Early Adulthood*; Beck, J. D., Bokemeyer, C., Langer, T., Eds.; Springer International Publishing: Cham, 2021; pp 401–415. https://doi.org/10.1007/978-3-030-49140-6_40.
- (13) Jardim, D. L.; De Melo Gagliato, D.; Nikanjam, M.; Barkauskas, D. A.; Kurzrock, R. Efficacy and Safety of Anticancer Drug Combinations: A Meta-Analysis of Randomized Trials with a Focus on Immunotherapeutics and Gene-Targeted Compounds. *Oncoimmunology* **2020**, 9 (1), 1710052. <https://doi.org/10.1080/2162402X.2019.1710052>.
- (14) Yu, W. Di; Sun, G.; Li, J.; Xu, J.; Wang, X. Mechanisms and Therapeutic Potentials of Cancer Immunotherapy in Combination with Radiotherapy and/or Chemotherapy. *Cancer Lett.* **2019**, 452, 66–70. <https://doi.org/10.1016/j.canlet.2019.02.048>.
- (15) Winkler, G. C.; Barle, E. L.; Galati, G.; Kluwe, W. M. Functional Differentiation of Cytotoxic Cancer Drugs and Targeted Cancer Therapeutics. *Regul. Toxicol. Pharmacol.* **2014**, 70 (1), 46–53. <https://doi.org/10.1016/j.yrtph.2014.06.012>.
- (16) Alderden, R. A.; Hall, M. D.; Hambley, T. W. The Discovery and Development of Cisplatin. *J. Chem. Educ.* **2006**, 83 (5), 728. <https://doi.org/10.1021/ed083p728>.

- (17) Todd, R. C.; Lippard, S. J. Inhibition of Transcription by Platinum Antitumor Compounds. *Metallomics* **2009**, *1* (4), 280–291. <https://doi.org/10.1039/b907567d>.
- (18) Wang, K.; Lu, J.; Li, R. The Events That Occur When Cisplatin Encounters Cells. *Coord. Chem. Rev.* **1996**, *151*, 53–88. [https://doi.org/10.1016/s0010-8545\(96\)90195-2](https://doi.org/10.1016/s0010-8545(96)90195-2).
- (19) Boros, E.; Dyson, P. J.; Gasser, G. Classification of Metal-Based Drugs According to Their Mechanisms of Action. *Chem* **2020**, *6* (1), 41–60. <https://doi.org/10.1016/j.chempr.2019.10.013>.
- (20) Kelland, L. R. Preclinical Perspectives on Platinum Resistance. *Drugs* **2000**, *59 Suppl 4*, 1–8. <https://doi.org/10.2165/00003495-200059004-00001>.
- (21) Decatris, M. P.; Sundar, S.; O'Byrne, K. J. Platinum-Based Chemotherapy in Metastatic Breast Cancer: Current Status. *Cancer Treat. Rev.* **2004**, *30* (1), 53–81. [https://doi.org/10.1016/S0305-7372\(03\)00139-7](https://doi.org/10.1016/S0305-7372(03)00139-7).
- (22) Ndagi, U.; Mhlongo, N.; Soliman, M. E. Metal Complexes in Cancer Therapy - an Update from Drug Design Perspective. *Drug Des. Devel. Ther.* **2017**, *11*, 599–616. <https://doi.org/10.2147/DDDT.S119488>.
- (23) Wani, W. A.; Baig, U.; Shreaz, S.; Shiekh, R. A.; Iqbal, P. F.; Jameel, E.; Ahmad, A.; Mohd-Setapar, S. H.; Mushtaque, M.; Ting Hun, L. Recent Advances in Iron Complexes as Potential Anticancer Agents. *New J. Chem.* **2016**, *40* (2), 1063–1090. <https://doi.org/10.1039/C5NJ01449B>.
- (24) Munteanu, C. R.; Suntharalingam, K. Advances in Cobalt Complexes as Anticancer Agents. *Dalton Trans.* **2015**, *44* (31), 13796–13808. <https://doi.org/10.1039/C5DT02101D>.
- (25) Huheey, J. E.; Keither, E. A.; Keiter, R. L. Coordination Chemistry: Structure. In *Inorganic chemistry: Principles of Structure and Reactivity*; New York, 1993; pp 472–536.

- (26) Hambley, T. W. Developing New Metal-Based Therapeutics: Challenges and Opportunities. *Dalton Trans.* **2007**, (43), 4929–4937. <https://doi.org/10.1039/B706075K>.
- (27) Abu-Dief, A. M.; Mohamed, I. M. A. A Review on Versatile Applications of Transition Metal Complexes Incorporating Schiff Bases. *Beni-Suef Univ. J. Basic Appl. Sci.* **2015**, 4 (2), 119–133. <https://doi.org/10.1016/j.bjbas.2015.05.004>.
- (28) Chen, T.; Li, M.; Liu, J. π – π Stacking Interaction: A Nondestructive and Facile Means in Material Engineering for Bioapplications. *Cryst. Growth Des.* **2018**, 18 (5), 2765–2783. <https://doi.org/10.1021/acs.cgd.7b01503>.
- (29) Khan, S.; Malla, A. M.; Zafar, A.; Naseem, I. Synthesis of Novel Coumarin Nucleus-Based DPA Drug-like Molecular Entity: In Vitro DNA/Cu(II) Binding, DNA Cleavage and pro-Oxidant Mechanism for Anticancer Action. *PLoS One* **2017**, 12 (8), e0181783. <https://doi.org/10.1371/journal.pone.0181783>.
- (30) Lawrance, G. A. The Central Atom. *Introduction to Coordination Chemistry*. January 22, 2010, pp 1–14. <https://doi.org/https://doi.org/10.1002/9780470687123.ch1>.
- (31) Jones, C.; Thornback, J. Chapter 4 Therapeutic Medicine. In *Medicinal Applications of Coordination Chemistry*; The Royal Society of Chemistry, 2007; pp 201–323. <https://doi.org/10.1039/9781847557759-00201>.
- (32) Frezza, M.; Hindo, S.; Chen, D.; Davenport, A.; Schmitt, S.; Tomco, D.; Dou, Q. P. Novel Metals and Metal Complexes as Platforms for Cancer Therapy. *Curr. Pharm. Des.* **2010**, 16 (16), 1813–1825. <https://doi.org/10.2174/138161210791209009>.
- (33) van Rijt, S. H.; Sadler, P. J. Current Applications and Future Potential for Bioinorganic Chemistry in the Development of Anticancer Drugs. *Drug Discov. Today* **2009**, 14 (23–24), 1089–1097. <https://doi.org/10.1016/j.drudis.2009.09.003>.
- (34) Kirubavathy, S. J.; Velmurugan, R.; Karvembu, R.; Bhuvanesh, N. S. P.;

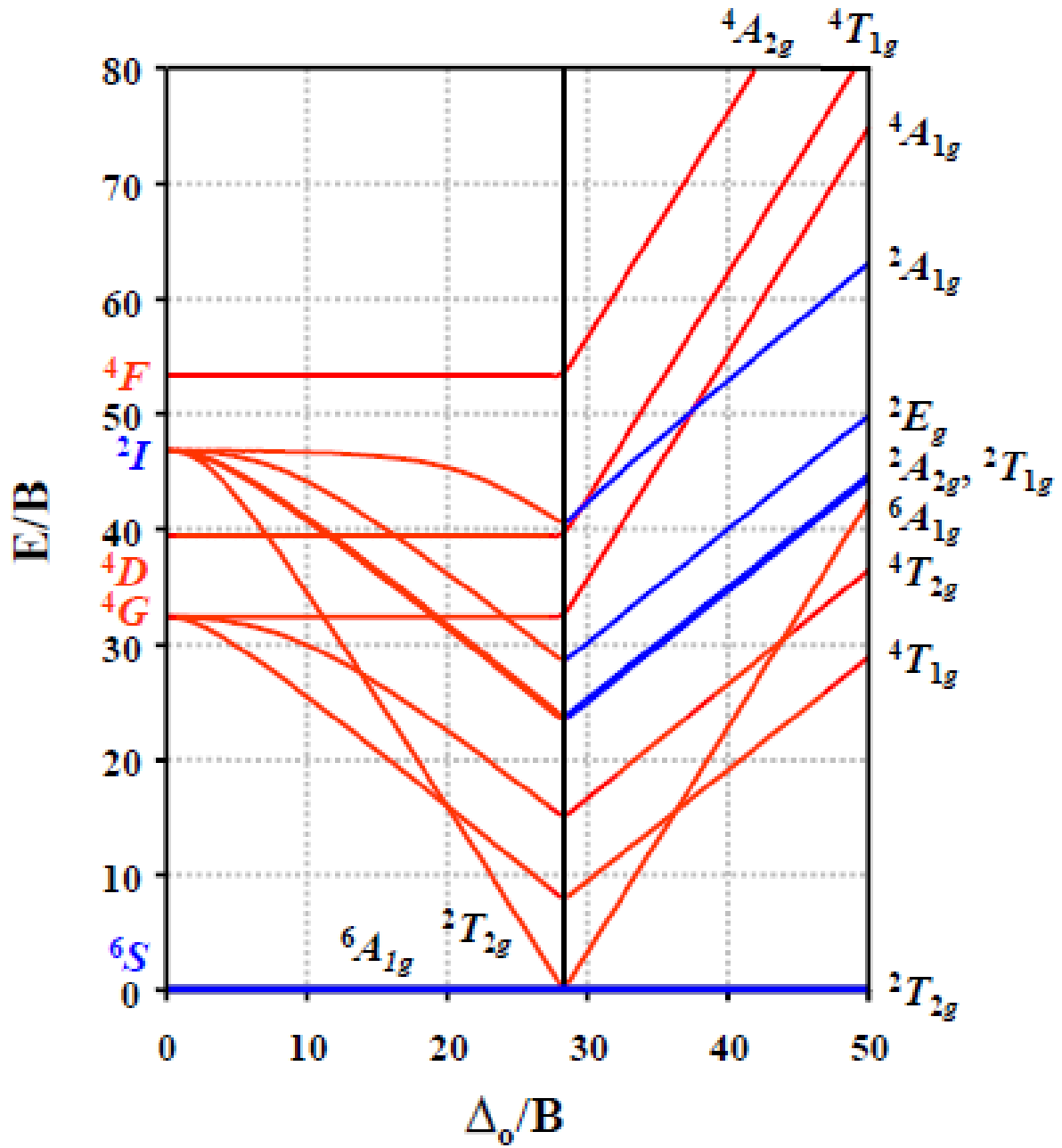
- Parameswari, K.; Chitra, S. Synthesis, Structure, and Pharmacological Evaluation of Co(III) Complex Containing Tridentate Schiff Base Ligand. *Russ. J. Coord. Chem.* **2015**, *41* (5), 345–352. <https://doi.org/10.1134/S1070328415050048>.
- (35) Swinney, D. C. Molecular Mechanism of Action (MMoA) in Drug Discovery. In *Annual Reports in Medicinal Chemistry*; Macor, J. E. B. T.-A. R. in M. C., Ed.; Academic Press, 2011; Vol. 46, pp 301–317. <https://doi.org/10.1016/B978-0-12-386009-5.00009-6>.
- (36) Ghanbari, Z.; Housaindokht, M. R.; Izadyar, M.; Bozorgmehr, M. R.; Eshtiagh-Hosseini, H.; Bahrami, A. R.; Matin, M. M.; Khoshkholgh, M. J. Structure-Activity Relationship for Fe(III)-Salen-Like Complexes as Potent Anticancer Agents. *Sci. World J.* **2014**, *2014*, 745649. <https://doi.org/10.1155/2014/745649>.
- (37) Basu, U.; Roy, M.; Chakravarty, A. R. Recent Advances in the Chemistry of Iron-Based Chemotherapeutic Agents. *Coord. Chem. Rev.* **2020**, *417*, 213339. <https://doi.org/10.1016/j.ccr.2020.213339>.
- (38) Janiak, C. A Critical Account on π – π Stacking in Metal Complexes with Aromatic Nitrogen-Containing Ligands. *J. Chem. Soc., Dalton Trans.* **2000**, (21), 3885–3896. <https://doi.org/10.1039/B003010O>.
- (39) Puntoriero, F.; Nastasi, F.; Galletta, M.; Campagna, S. Photophysics and Photochemistry of Non-Carbonyl-Containing Coordination and Organometallic Compounds. In *Comprehensive Inorganic Chemistry II (Second Edition): From Elements to Applications*; Reedijk, J., Poeppelmeier, K. B. T.-C. I. C. I. I. (Second E., Eds.; Elsevier: Amsterdam, 2013; Vol. 8, pp 255–337. <https://doi.org/10.1016/B978-0-08-097774-4.00802-0>.
- (40) Farrer, N. J.; Salassa, L.; Sadler, P. J. Photoactivated Chemotherapy (PACT): The Potential of Excited-State d-Block Metals in Medicine. *Dalton Trans.* **2009**, (48), 10690–10701. <https://doi.org/10.1039/b917753a>.
- (41) Tyler, D. R. Organometallic Photochemistry, Synthetic Aspects and Applications. In *Comprehensive Organometallic Chemistry III*; Mingos, D. M. P., Crabtree, R. H.

- B. T.-C. O. C. I. I. I., Eds.; Elsevier: Oxford, 2007; Vol. 1, pp 239–262.
<https://doi.org/10.1016/b0-08-045047-4/00010-8>.
- (42) Agrawal, S. Nucleic Acid Extraction. In *Techniques in Molecular Biology*; International Book Distributing Company, 2008; pp 1–53.
- (43) Jenkins, T. C. Optical Absorbance and Fluorescence Techniques for Measuring DNA-Drug Interactions. *Methods Mol. Biol.* **1997**, *90*, 195–218.
<https://doi.org/10.1385/0-89603-447-X:195>.
- (44) Carver, P. L.; Meunier, B.; Robert, A.; Crisponi, G.; Nurchi, V.; Lachowicz, J. I.; Nairz, M.; Weiss, G.; Pai, A. B.; Ward, R. J.; Others. COBALT-SCHIFF BASE COMPLEXES: PRECLINICAL RESEARCH AND POTENTIAL THERAPEUTIC USES. In *Essential Metals in Medicine: Therapeutic Use and Toxicity of Metal Ions in the Clinic*; De Gruyter, 2019; pp 267–301. <https://doi.org/doi:10.1515/9783110527872>.
- (45) Prieto-Martínez, F. D.; Arciniega, M.; Medina-Franco, J. L. Molecular Docking: Current Advances and Challenges. *TIP Revista Especializada en Ciencias Químico-Biológicas*. scielomx 2018, pp 65–87.
<https://doi.org/10.22201/fesz.23958723e.2018.0.143>.
- (46) Morris, G. M.; Huey, R.; Lindstrom, W.; Sanner, M. F.; Belew, R. K.; Goodsell, D. S.; Olson, A. J. AutoDock4 and AutoDockTools4: Automated Docking with Selective Receptor Flexibility. *J. Comput. Chem.* **2009**, *30* (16), 2785–2791.
<https://doi.org/10.1002/jcc.21256>.
- (47) Agrawal, P.; Singh, H.; Srivastava, H. K.; Singh, S.; Kishore, G.; Raghava, G. P. S. Benchmarking of Different Molecular Docking Methods for Protein-Peptide Docking. *BMC Bioinformatics* **2019**, *19* (13), 426. <https://doi.org/10.1186/s12859-018-2449-y>.
- (48) Khusro, A.; Aarti, C.; Agastian, P. Computational Modelling and Docking Insight of Bacterial Peptide as Ideal Anti-Tubercular and Anticancer Agents. *Biocatal. Agric. Biotechnol.* **2020**, *26*, 101644.
<https://doi.org/https://doi.org/10.1016/j.bcab.2020.101644>.

- (49) Ruiz, K. A.; López, M.; Suppan, G.; Makowski, K. Crossed Aldol Reactions in Water Using Inexpensive and Easily Available Materials as a Tool for Reaction Optimization Teaching in an Undergraduate Organic Chemistry Laboratory. *J. Chem. Educ.* **2020**, *97* (10), 3806–3809. <https://doi.org/10.1021/acs.jchemed.0c00519>.
- (50) Ambika, S.; Manojkumar, Y.; Arunachalam, S.; Gowdhami, B.; Meenakshi Sundaram, K. K.; Solomon, R. V.; Venuvanalingam, P.; Akbarsha, M. A.; Sundararaman, M. Biomolecular Interaction, Anti-Cancer and Anti-Angiogenic Properties of Cobalt(III) Schiff Base Complexes. *Sci. Rep.* **2019**, *9* (1), 2721. <https://doi.org/10.1038/s41598-019-39179-1>.
- (51) Shreaz, S.; Sheikh, R. A.; Bhatia, R.; Neelofar, K.; Imran, S.; Hashmi, A. A.; Manzoor, N.; Basir, S. F.; Khan, L. A. Antifungal Activity of α -Methyl Trans Cinnamaldehyde, Its Ligand and Metal Complexes: Promising Growth and Ergosterol Inhibitors. *Biometals an Int. J. role Met. ions Biol. Biochem. Med.* **2011**, *24* (5), 923–933. <https://doi.org/10.1007/s10534-011-9447-0>.
- (52) Langford, C. H.; Chung, F. M. Mechanism of Complex Formation and Solvent-Exchange Reactions of Iron(3+) in Dimethyl Sulfoxide. *J. Am. Chem. Soc.* **1968**, *90* (16), 4485–4486. <https://doi.org/10.1021/ja01018a067>.
- (53) Marcos-Merino, J. M.; Gallego, R. E.; de Alda, O.; Gómez, J. Extracción de ADN Con Material Cotidiano: Desarrollo de Una Estrategia Interdisciplinar a Partir de Sus Fundamentos Científicos. *Educ. química* **2019**, *30* (1), 58–69. <https://doi.org/10.22201/fq.18708404e.2019.1.65732>.
- (54) Burt, S. Essential Oils: Their Antibacterial Properties and Potential Applications in Foods--a Review. *Int. J. Food Microbiol.* **2004**, *94* (3), 223–253. <https://doi.org/10.1016/j.ijfoodmicro.2004.03.022>.
- (55) Pavia, D. L.; Lampman, G. M.; Kriz, G. S.; Vyvyan, J. A. Infrared Spectroscopy. In *Introduction to Spectroscopy*; Cengage Learning, 2015; pp 14–106.
- (56) Khan, M.; Khan, N.; Ghazal, K.; Shoaib, S.; Samiullah; Ali, I.; Rauf, M. K.; Badshah,

- A.; Tahir, M. N.; Rehman, A.-U. Synthesis, Characterization, Crystal Structure, in-Vitro Cytotoxicity, Antibacterial, and Antifungal Activities of Nickel(II) and Cobalt(III) Complexes with Acylthioureas. *J. Coord. Chem.* **2020**, *73* (12), 1790–1805. <https://doi.org/10.1080/00958972.2020.1793136>.
- (57) Nakamoto, K. Applications in Coordination Chemistry. *Infrared and Raman Spectra of Inorganic and Coordination Compounds*. December 30, 2008, pp 1–273. <https://doi.org/10.1002/9780470405888.ch1>.
- (58) Kovacic, J. E. The C=N Stretching Frequency in the Infrared Spectra of Schiff's Base Complexes-I. Copper Complexes of Salicylidene Anilines. *Spectrochim. Acta Part A Mol. Spectrosc.* **1967**, *23* (1), 183–187. [https://doi.org/10.1016/0584-8539\(67\)80219-8](https://doi.org/10.1016/0584-8539(67)80219-8).
- (59) Khalaji, A. D.; Das, D. Studies on Co(II) and Cu(II) Complexes of a Ligand Derived from 1,3-Phenylenediamine and 5-Bromosalicylaldehyde Synthesis, Characterisation, Thermal Properties and Use as New Precursors for Preparation Cobalt and Copper Oxide Nano-Particles. *J. Therm. Anal. Calorim.* **2013**, *114* (2), 671–675. <https://doi.org/10.1007/s10973-013-2974-x>.
- (60) Nakamoto, K. Appendixes. *Infrared and Raman Spectra of Inorganic and Coordination Compounds*. December 31, 2008, pp 355–413. <https://doi.org/10.1002/9780470405840.app1>.
- (61) Abbas, N. K.; Habeeb, M. A.; Algidsawi, A. J. K. Preparation of Chloro Penta Amine Cobalt(III) Chloride and Study of Its Influence on the Structural and Some Optical Properties of Polyvinyl Acetate. *Int. J. Polym. Sci.* **2015**, *2015*, 926789. <https://doi.org/10.1155/2015/926789>.
- (62) Ray, A.; Banerjee, S.; Butcher, R. J.; Desplanches, C.; Mitra, S. Two New End-on Azido Bridged Dinuclear Copper(II) and Cobalt(III) Complexes Derived from the (E)-N'-((Pyridin-2-Yl)Methylene) Acetohydrazide Schiff Base Ligand: Characterisation, Crystal Structures and Magnetic Study. *Polyhedron* **2008**, *27* (11), 2409–2415. <https://doi.org/https://doi.org/10.1016/j.poly.2008.04.018>.

- (63) Murray, M. G.; Thompson, W. F. Rapid Isolation of High Molecular Weight Plant DNA. *Nucleic Acids Res.* **1980**, *8* (19), 4321–4325. <https://doi.org/10.1093/nar/8.19.4321>.
- (64) Bain, G. A.; Berry, J. F. Diamagnetic Corrections and Pascal's Constants. *J. Chem. Educ.* **2008**, *85* (4), 532. <https://doi.org/10.1021/ed085p532>.
- (65) Kundu, P. P. Conformational Analysis of Molecules: Combined Vibrational Spectroscopy and Density Functional Theory Study; Stauffer, C. N. E.-M. T., Ed.; IntechOpen: Rijeka, 2016; p Ch. 9. <https://doi.org/10.5772/64452>.
- (66) Parsons, D. G.; Truter, M. R.; Wingfield, J. N. Alkali Metal Tetraphenylborate Complexes with Some Macrocyclic, "Crown", Polyethers. *Inorganica Chim. Acta* **1975**, *14*, 45–48. [https://doi.org/https://doi.org/10.1016/S0020-1693\(00\)85720-5](https://doi.org/https://doi.org/10.1016/S0020-1693(00)85720-5).
- (67) Mohamed, M. A.; Jaafar, J.; Ismail, A. F.; Othman, M. H. D.; Rahman, M. A. Chapter 1 Fourier Transform Infrared (FTIR) Spectroscopy; 2021; pp 3–29. <https://doi.org/10.1016/b978-0-444-63776-5.00001-2>.
- (68) Cotton, F. A.; Francis, R.; Horrocks, W. D. SULFOXIDES AS LIGANDS. II. THE INFRARED SPECTRA OF SOME DIMETHYL SULFOXIDE COMPLEXES. *J. Phys. Chem.* **1960**, *64* (10), 1534–1536. <https://doi.org/10.1021/j100839a046>.

d^5 Tanabe-Sugano Diagram

d^6 Tanabe-Sugano Diagram

